Chapter 7
Diamond Surgical Tools

H. Sein, C. Maryan, A. Jones, J. Verran, N. Ali, I.U. Hassan, C. Rego, W. Ahmed and M.J. Jackson

Abstract Deposition technology has played a major part in the creation of today's scientific devices. Computers, electronic equipment, biomedical implants, cutting tools, optical components, and automotive parts are all based on material structures created by thin film deposition processes. There are many coating processes ranging from the traditional electroplating to the more advanced laser or ion-assisted deposition. However, the choice of deposition technology depends upon many factors including substrates properties, component dimensions and geometry, production requirements, and the exact coating specification needed for the application of interest. For complex geometry components, small feature sizes, good reproducibility, and high product throughput, chemical vapor deposition (CVD) is a highly effective technology. For example, low pressure and plasma-assisted CVD is a well-established technology for semiconductor devices, which has very small feature sizes and complex geometrical arrangements on the surface.

7.1 Introduction

In order to understand both physical vapor deposition (PVD) and chemical vapor deposition (CVD) processes, one has to model them in terms of several steps. These processes can be divided into the following stages:

- **Generation of Vapor Phase Species**

The precursor materials are converted into a convenient form so that transport to the substrates is efficient. Vapor is generated in the reactor. Hot filaments, lasers,

H. Sein · C. Maryan · A. Jones · J. Verran · N. Ali · I.U. Hassan · C. Rego
Manchester Metropolitan University, Manchester, UK

W. Ahmed
School of Medicine, University of Central Lancashire, Preston, UK

M.J. Jackson (✉)
Kansas State University, Salina, KS, USA
e-mail: jacksonmj04@yahoo.com

W. Ahmed and M.J. Jackson (eds.), *Surgical Tools and Medical Devices*,
DOI 10.1007/978-3-319-33489-9_7

microwave, ion beams, electron guns, etc., can be used to activate the source materials, enabling deposition to be carried out.

- **Transport of Source Materials to the Substrate Region**

The vapor species are transported from the source to the substrate with or without collision between the atoms and molecules. During transport, some of the species can be ionized by creating plasma in this space. This is normally carried out in a vacuum system; however, atmospheric CVD systems are also employed.

- **Adsorption of Active Species on the Substrate Surface**

For deposition to take place, the active species must first be adsorbed onto the active sites on the surfaces. Initially, this occurs via physisorption where the species adhere to the surface with weak van der Waals forces and then strong covalent bonds are formed between the species and the surface known as chemisorption.

- **Decomposition Adsorbed Species on the Substrate Surface**

Once the gaseous species are adsorbed onto surface site and the energy of the species is sufficient then decomposition of the precursors can take place resulting in the creation of nucleation center.

- **Nucleation and Film Formation**

The process involves the subsequent formation of the film via nucleation and growth processes. These can be strongly influenced by process parameters resulting in a change in the microstructure, composition, impurities, and residual stress of the films. The final film properties are highly dependent on the microstructural and interfacial characteristics of the deposited coating.

Independent control of these stages is critical and determines the versatility or flexibility of deposition process. For example, PVD process parameters can be independently and precisely monitored and controlled; thus allowing microstructure, properties, and deposition rates to be tailored specifically to the performance requirements of the product. Generally, CVD processes have the advantage of good throwing power enabling complex geometry substrates to be coated, while the deposition rates in PVD processes are much higher than those in CVD processes at lower deposition temperatures.

Although CVD and PVD processes are simple in principle, one must be well versed in vacuum technology, physics, chemistry, material science, mechanical, and electrical engineering as well as in elements of thermodynamics, chemical kinetics, surface mobility, and condensation phenomena in order to obtain a detailed fundamental understanding of these processes. In this chapter, we restrict our attention to the deposition of diamond thin films for use in cutting tools.

Table 7.1 Properties of diamond

Properties	Applications
High wear resistance	Cutting tools
Chemical inertness	Electrochemical sensors
High thermal conductivity	Heat spreaders
Biological inertness	In vitro applications
Semiconducting when doped	Electronic devices
High resistivity (insulator)	Electronic devices
Negative electron affinity	Cold cathode electron sources

7.2 Properties of Diamond

Diamond is an advanced material with an excellent combination of physical and chemical properties. If high-quality diamond films with comparable properties to natural diamond can be formed with low surface roughness, numeral potential applications will emerge in the near future particularly in the emerging field of nanotechnology.

Diamond as a material possesses a remarkable range of physical attributes, which make it a promising material for a large range of applications. Selections of these are given in Table 7.1. However, owing to the cost and availability of large natural diamonds, most of these applications have not been developed to their full potential.

7.3 History of Diamond

7.3.1 Early History of Diamond Synthesis

Diamond is one of the most technologically and scientifically valuable crystalline solids found in nature. Their unique blends of properties are effectively incomparable to any other known material. Sir Isaac Newton was the first to characterize diamond and determine it to be of organic origin while in 1772, the French chemist Antoine L. Lavoisier established that the product of diamond combustion was limited to carbon dioxide.

English chemist Smithson Tennant showed that diamond combustion products were no different than those of coal or graphite and resulted in “bound air.” Later, the discovery of X-rays enabled Sir William Henry Bragg and his son Sir William Lawrence Bragg to determine that carbon allotropes were cubic (diamond), hexagonal (graphite), and amorphous. With this information, early attempts to synthesize diamond began in France in 1832 with C.C. de la Tour and later in England by J.B. Hanney and H. Moisson. The results of their work are disputed to this day.

Synthesis of diamond has attracted widespread attention ever since it was established; that diamond is a crystalline form of carbon. Since diamond is the densest carbon phase, it became immediately plausible that pressure, which produces a smaller volume and therefore a higher density, may convert other forms of carbon into diamond. As understanding of chemical thermodynamics developed throughout the nineteenth and twentieth centuries, the pressure–temperature range of diamond stability was explored. In 1955, these efforts culminated in the development of a high pressure–high temperature (HPHT) process of diamond synthesis with a molten transition metal solvent-catalyst at pressures where diamond is the thermodynamically stable phase [1]. Three major problems can be isolated for emphasizing the difficulty of making diamond in the laboratory. First, there is difficulty in achieving the compact and strongly bonded structure of diamond, which requires extreme pressure. Second, even when such a high pressure has been achieved, a very high temperature is required to make the conversion from other forms of carbon to diamond proceed at a useful rate. Finally, when diamond is thus obtained, it is in the form of very small grains and to achieve large single crystal diamond requires yet another set of constraints. However, less well known has been a parallel effort directed toward the growth of diamond at low pressures where it is metastable. Metastable phases can form from precursors with high chemical potential if the activation barriers to more stable phases are sufficiently high. As the precursors fall in energy, they can be trapped in a metastable configuration. Formation of a metastable phase depends on selecting conditions in which rates of competing processes to undesired products are low [2]. In the case of diamond, achieving the appropriate conditions has taken decades of research [3]. The processes competing with diamond growth are spontaneous graphitization of the diamond surface as well as nucleation and growth of graphitic deposits.

The most successful process for low-pressure growth of diamond has been CVD from energetically activated hydrocarbon/hydrogen gas mixtures. CVD is a process whereby a thin solid film, by definition, is synthesized from the gaseous phase via a chemical reaction. The development of CVD is common with many technologies and has been closely linked to the practical needs of society. The oldest example of a material deposited by CVD is probably that of pyrolytic carbon, since as Ashfold et al. [4] pointed out, some prehistoric art was done on cave walls with soot condensed from the incomplete oxidation of firewood. A similar procedure formed the basis of one of the earliest patents and commercial exploitation of a CVD process, which was issued for the preparation of carbon black as a pigment. The emerging electric lamp industry provided the next major application of CVD with a patent issued for improvements to fragile carbon filaments [4]. Since these improved filaments were far from robust, the future for a pyrolytic carbon CVD industry was limited and a few years later, processes for the deposition of metals to improve the quality of lamp filaments were described [5]. From the turn of the century through to the late 1930s, a variety of techniques appeared for the preparation of refractory metals for a number of applications. It was also during this period that silicon was first deposited by hydrogen reduction of silicon tetrachloride [5] and the use of that material for electronic applications was foreseen by the

development of silicon-based photo cells [6] in 1946 as well as rectifiers [7]. The preparation of high-purity metals, various coatings, and electronic materials has developed significantly in the past 45 years or so, but it is undoubtedly the demand and requirement of the semiconductor and microelectronic industries that have been the main driving force in the development of CVD techniques as well as the greater efforts for understanding the basics of CVD processes. Consequently, a large body of literature and reviews now exist on CVD.

Indeed, it was the CVD from carbon-containing gases that enabled W.G. Eversole, referred to in reference [8], at the Union Carbide Corporation, to be the first to grow diamond successfully at low pressures in 1952, after which conclusive proof and repetition of the experiments took place. In the initial experiments, carbon monoxide was used as a source gas to precipitate diamond on a diamond seed crystal. However, in subsequent experiments, methane and other carbon-containing gases were used as well as a cyclic growth etches procedure to remove co-deposited graphite. In all of his studies, it was necessary to use diamond seeds in order to initiate diamond growth. The deposits were identified as diamond by density measurements, chemical analysis, and diffraction techniques. The synthesis by Eversole preceded the successful diamond synthesis at high pressure by workers at the General Electric Company [1], which was accomplished in 1954. However, the important difference was that Eversole grew diamond on preexisting diamond nuclei whereas the general electric syntheses did not initiate growth on diamond seed crystals. Angus [9], Yarbrough and Messier [10], in the former Soviet Union, began work on low-pressure diamond synthesis in 1956, in which many approaches were taken, which started with the growth of diamond whiskers by a metal-catalyzed vapor–liquid–solid process. Subsequently, epitaxial growth from hydrocarbons and hydrocarbon/hydrogen mixtures was investigated as well as different forms of vapor transport reactions. In addition, theoretical investigations of the relative nucleation rates of diamond and graphite were also performed. Angus and co-workers at Case Western Reserve University concentrated primarily on diamond CVD on diamond seed crystals from hydrocarbons and hydrocarbon/hydrogen mixtures [11, 12]. They grew *p*-type semiconducting diamond from methane/diborane gas mixtures and studied the rates of diamond and graphite growth in methane/hydrogen gas mixtures and ethylene. They were the first to report on the preferential etching of graphite compared to diamond by atomic hydrogen and noted that boron had an unusual catalytic effect on metastable diamond growth.

The role of hydrogen in permitting metastable diamond growth was also recognised by some early workers. The low-energy electron diffraction (LEED) study of Spear [13] and Kamo et al. [14] showed that a {111}-diamond surface saturated with hydrogen gave an unreconstructed (1 × 1) LEED pattern. The unsatisfied dangling bonds normal to the surface are terminated with hydrogen atoms, which maintain the bulk terminated diamond lattice to the outermost surface layer of carbon atoms. When hydrogen is absent, the surface reconstructs into more complex structures. They also showed that carbon atoms are very mobile on the diamond surface at temperatures above 1200 K and stated that these conditions should permit epitaxial growth. Other work [15, 16] suggested that the presence of

hydrogen enhanced diamond growth. Williams et al. [17] and Kobashi et al. [18] as well as Liou et al. [19] showed that addition of hydrogen to the hydrocarbon gas phase suppressed the growth rate of graphite relative to diamond thus resulting in higher diamond yields. Eventually, however, graphitic carbons nucleated on the surface and suppressed further diamond growth. It was then necessary to remove the graphitic deposits preferentially with atomic hydrogen [20] or oxygen [21], and to repeat the sequence. By the mid-1970s, diamond growth at low pressures had been achieved by several groups. The beneficial role of hydrogen was known to some extent and growth rates of 0.1 μm h^{-1} had been achieved. Although the growth rates were too low to be of any commercial importance, the results provided the experimental foundation for much of the work that followed.

7.3.2 Metastable Diamond Growth

Japanese researchers associated with the National Institute for Research in Inorganic Materials (NIRIM) made the first disclosure of methods for rapid diamond growth at low pressures. Research on metastable diamond growth was initiated at NIRIM in 1974. In 1982, they described techniques for synthesizing diamond at rates of several microns per hour from gases decomposed by a hot filament as well as microwave or DC discharges [22–25]. These processes produced individual faceted crystals without the use of a diamond seed crystal. The current worldwide interest in new diamond technology can in fact be directly traced to the NIRIM effort. Although Deryagin, as reported in reference [26], had reported high-rate diamond growth earlier, process details were not disclosed [26]. All the techniques are based on the generation of atomic hydrogen in the vicinity of the growth surface during deposition. Although the CVD of diamond from hydrogen-rich/hydrocarbon-containing gases has been the most successful method of diamond synthesis, numerous other methods have been attempted with varying degrees of success, with ion beam methods being the most successful [27]. In 1971, hard carbon films were first deposited using a beam of carbon ions. As the films had many of the properties of diamond, they were called diamond-like carbon because definitive diffraction identification was not possible. In 1976, Akatsuka et al. [28] formed finely divided polycrystalline diamond (PCD) using a beam of carbon ions with energies between 50 and 100 eV, and subsequently Suzuki et al. [29] grew diamond via ion implantation.

With further research and additional technological progress in improving and devising new methods for synthesis and fabrication, it becomes increasingly likely that new applications will be discovered. In order to be able to take full advantage of the unique characteristics of diamond as a material for the construction of solid-state devices, basic scientific understanding of the various experimental process techniques and in particular the introduction and activation of dopants must be obtained. Attention also needs to be paid to proper design of devices incorporating novel features utilizing concepts and practices established in silicon and

gallium arsenide device technology. The potential of diamond as a material for solid-state devices has been the subject of a few reviews [8, 30–35] that have discussed the electronic material parameters of diamond and the simulated characteristics that can be obtained. Simple devices incorporating diamond have been demonstrated primarily incorporating natural or HPHT diamond. Photodetectors, light-emitting diodes, nuclear radiation detectors, thermistors, varistors, and negative resistance devices in synthetic crystals have been demonstrated. Several groups [36–40] have also demonstrated basic field effect transistor device operation in epitaxial diamond films and boron-doped layers on single crystal diamond substrates. However, for wide application of diamond solid-state devices, high-quality films on more commonly available substrates are essential as well as studies on the device potential of polycrystalline films. So far, only thermistors [41] and Schottky diodes [42] have been produced and characterized in the polycrystalline material. This is due to material problems; in that the polycrystalline nature of the films result in grain boundaries, twins, stacking faults, and other defects, which have restricted exploitation in the electronic industries. To date, there have been no confirmed observations of a means of achieving heteroepitaxy, i.e., single crystal diamond grown on a non-diamond substrate, and therefore no means of achieving diamond devices for practical applications. Indeed, achieving heteroepitaxy stands as the single most prominent technological hurdle for diamond-based electronics. However, CVD synthesis is a very active area that is improving with experience. In the near future, in situ probes may be used to optimize various diamond CVD processes by providing a maximization of the flow of diamond precursors to the surface while simultaneously minimizing the competing deposition of non-diamond carbon forms. The wide variety of means by which diamond is being routinely formed as a film will enhance its deployment and the potential for active electronic exploitation. Indeed, diamond coatings in general are expected to make so large an impact in the future that many people believe that the future age will be known as the diamond age, going chronologically from the Stone Age and Bronze Age, to the Iron Age of the past and the Silicon Age of the present.

7.4 CVD Diamond Technology

The reactor system (comprising the reaction chamber and all associated equipment) for carrying out CVD) processes must provide several basic functions common to all type of systems (Fig. 7.1). It must allow transport of the reactant and diluents gases to the reaction site, provide activation energy to the reactants (heat, radiation, plasma), maintain a specific system pressure and temperature, allow the chemical processes for film deposition to proceed optimally, and remove the by-product gases and vapors. These functions must be implemented with adequate control, maximal effectiveness, and complete safety.

CVD is a crystal growth process used not only for diamond but also for a range of different semiconductor and other crystalline materials such as silicon or gallium

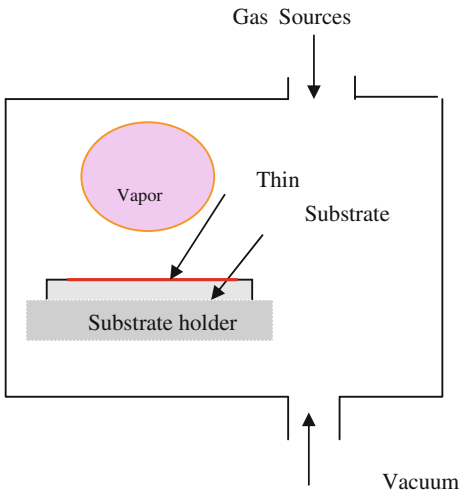

Fig. 7.1 A simple schematic of a vapor deposition process

arsenide. These industrial fields are diverse and range from gas turbines to gas cookers and from coinage to nuclear power plants.

The CVD process relies first on the generation of a species that is produced by the reaction of the element that is to be deposited with another element that results in the substantial increase in the depositing elements' vapor pressure. Second, this volatile species is then passed over or allowed to come into contact with the substrate being coated. This substrate is held at an elevated temperature, typically from 800 to 1150 °C. Finally, the deposition reaction usually occurs in the presence of a reducing atmosphere, such as hydrogen. The film properties can be controlled and modified by varying the problem parameters associated with the substrate, the reactor, and gas composition.

7.5 CVD Diamond Processes

Several different approaches to the deposition of diamond have been investigated and these include the ones described in the following sections.

7.5.1 Plasma-Enhanced CVD

Plasmas generated by various forms of electrical discharges or induction heating have been employed in the growth of diamond. The role of the plasma is to generate atomic hydrogen and to produce the necessary carbon precursors for diamond growth. The efficiencies of the different plasma processes vary from method to

method. Three plasma frequency regimes will be discussed. These are microwave plasma CVD, which typically uses excitation frequencies of 2.45 GHz; Radio-frequency (RF) plasma excitation, which employs frequencies of usually 13.56 MHz; and direct-current (DC) plasmas, which can be run at low electric powers (a "cold" plasma) or at high electric powers (which create an *arc* or a *thermal* plasma).

RF Plasma-Enhanced CVD

Generally, RF power can be applied to create plasma in two electrode configurations, namely, in an inductively coupled or a capacitively coupled parallel plate arrangement. A number of workers have reported the growth of diamond crystals and thin films using inductively coupled RF plasma methods [21–24] as well as capacitively coupled methods [25, 26]. A high power in the discharge leading to greater electron densities was found to be necessary for efficient diamond growth. However, the use of higher power results in physical and chemical sputtering from the reactor walls, leading to contamination of the diamond films [21]. The advantage of RF plasmas is that they can easily be generated over much larger areas than microwave plasmas but the method is not routinely applied for the deposition of diamond films.

DC Plasma-Enhanced CVD

In this method, plasma in a H_2-hydrocarbon mixture is excited by applying a DC bias across two parallel plates, one of which is the substrate [27–29]. DC plasma-enhanced CVD has the advantage of being able to coat large areas as the diamond deposition area is limited by the electrodes and the DC power supply. In addition, the technique has the potential for very high growth rates. However, diamond films produced by DC plasmas were reported to be under high stress and to contain high concentrations of hydrogen as well as impurities resulting from plasma erosion of the electrodes.

Microwave Plasma-Enhanced CVD

Microwave plasma-assisted CVD has been used more extensively than any other method for the growth of diamond films [14–20]. Microwave plasmas are different from other plasmas in that the microwave frequency can oscillate electrons. Collision of electrons with gaseous atoms and molecules generate high ionization fractions. This method of diamond film growth has a number of distinct advantages over the other methods of diamond film growth. Microwave deposition, being an electrodeless process, avoids contamination of the films due to electrode erosion. Furthermore, the microwave discharge at 2.45 GHz, being a higher frequency process than the RF discharges at typically 13.56 MHz, produces a higher plasma density with higher energy electrons, which effectively results in higher concentrations of atomic hydrogen and hydrocarbon radicals leading to efficient diamond growth. In addition, as the plasma is confined to the center of the deposition chamber as a ball, carbon deposition onto the walls of the chamber is prevented.

7.5.2 Hot Filament CVD (HFCVD)

In the early 1970s, it was suggested that the simultaneous production of atomic hydrogen during hydrocarbon pyrolysis may enhance the deposition of diamond. Soviet researchers who generated H by dissociating H_2 using an electric discharge or a hot filament tested this suggestion [8]. It was observed that atomic hydrogen could easily be produced by the passage of H_2 over a refractory metal filament, such as tungsten, heated to temperatures between 2000 and 2500 K. When atomic hydrogen was added to the hydrocarbon, typically with a C/H ratio of ~ 0.01, it was observed that diamond could be deposited while graphite formation was suppressed. The generation of atomic hydrogen during diamond CVD enabled (a) a dramatic increase in the diamond deposition rate to approximately 1 μm h^{-1} and (b) the nucleation and growth of diamond on non-diamond substrates [8–13]. Because of its inherent simplicity and comparatively low operating cost, HFCVD has become very popular in the industry. Table 7.2 outlines typical deposition parameters used in the growth of diamond films by this technique.

A wide variety of refractory materials have been used as filaments including tungsten, tantalum, and rhenium due to their high electron emissivity. Refractory metals, which form carbides (e.g., tungsten and tantalum), typically must carburize their surface before supporting the deposition of diamond films. The process of filament carburization results in the consumption of carbon from the CH_4, and thus a specific incubation time is needed for the nucleation of diamond films. Therefore, this process may affect the early stages of film growth, although it is insignificant over longer periods. Furthermore, the volume expansion due to carbon incorporation leads to cracks along the length of the wire. The development of these cracks is undesirable, as it reduces the lifetime of the filament.

It is believed that thermodynamic near-equilibrium is established in the gas phase at the filament surface. At temperatures around 2300 K, molecular hydrogen dissociates into atomic hydrogen and methane transforms into methyl radicals, acetylene species, and other hydrocarbons stable at these elevated temperatures. Atomic hydrogen and the high-temperature hydrocarbons then diffuse from the filament to the substrate surface. Although the gaseous species generated at the filament are in equilibrium at the filament temperature, the species are at a super equilibrium concentration when they arrive at the much cooler substrate. The reactions that generate these high-temperature species (e.g., C_2H_2), at the surface of the filament or anywhere where there are hydrogen atoms, proceed faster than any

Table 7.2 Typical deposition parameters used in the growth of diamond films by HFCVD

Gas mixture	Total pressure (Torr)	Substrate temperature (K)	Filament temperature (K)
CH_4 (0.5–2.0 %)/H_2	10–50	1000–1400	2200–2500

reactions that decompose these species during the transit time from the filament to the substrate. Consider the equilibrium between methane and acetylene

$$2CH_4 \rightleftarrows C_2H_2 + 3H_2$$

At the filament surface, the reaction is immediately driven to the right, creating acetylene. After acetylene diffuses to the substrate, thermodynamic equilibrium at a substrate temperature of $\sim$1100 K calls for the formation of methane, but the reverse reaction proceeds much slower. Solid carbon precipitates on the substrate in order to reduce the superequilibrium concentration of species such as acetylene in the gas phase. The diamond allotrope of carbon is "stabilized" by a concurrent super equilibrium concentration of atomic hydrogen. This simple explanation emphasizes the importance of reaction kinetics in diamond synthesis by HFCVD.

Advantages of the CVD Process

The process is gas phase in nature, and therefore given a uniform temperature within the coating retort and likewise uniform concentrations of the depositing species the deposition rate will be similar on all surfaces. Therefore, variable- and complex-shaped surfaces, given reasonable access to the coating powders or gases, such as screw threads, blind holes, or channels or recesses, can be coated evenly without build-up on edges.

Disadvantages of the CVD Process

The CVD process is carried out at relatively high temperatures and therefore limitations due to dimensional tolerances are an important consideration. Components that have tight dimensional tolerances will not be amenable to CVD. However, the reduction of distortion during coating can sometimes be controlled by careful stress relieving after rough machining of the component during fabrication.

7.6 Treatment of Substrate

7.6.1 Selection of Substrate Material

Deposition of adherent high-quality diamond films onto substrates such as cemented carbides, stainless steel, and various metal alloys containing transition element has proved to be problematic. In general, the adhesion of the diamond films to the substrates is poor and the nucleation density is very low [43–50]. Mainly, refractory materials such as W (WC-Co), Mo, and Si have been used as substrate materials. Materials that form carbide are found to support diamond growth. However, materials such as Fe and steel possess a high mutual solubility with carbon, and only graphitic deposits or iron carbide result during CVD growth on these materials. For applications in which the substrate needs to remain attached to the CVD diamond film, it is necessary to choose a substrate that has a similar

Table 7.3 Solubility and diffusion rates of carbon atoms in different metals at 900 °C

	α-Fe	γ-Fe	Co	Ni
Solubility of carbon (wt%)	1.3	1.3	0.1	0.2
Carbon diffusion rate (cm/s)	2.35×10^{-6}	1.75×10^{-8}	2.46×10^{-8}	1.4×10^{-8}

thermal expansion coefficient to that of diamond. If this is not done, the stress caused by the different rates of contraction on cooling after deposition will cause the film to delaminate from the substrate. The influence of different metallic substrates on the diamond deposition process has been examined. Interactions between substrate materials and carbon species in the gas phase are found to be particularly important and lead to either carbide formation or carbon dissolution. Carbides are formed in the presence of carbon-containing gases on metals such as molybdenum, tungsten, niobium, hafnium, tantalum, and titanium. The carbide layer formed allows diamond to form on it since the minimum carbon surface concentration required for diamond nucleation cannot be reached on pure metals. As the carbide layer increases in thickness, the carbon transport rate to the substrate decreases until a critical level is reached where diamond is formed [51–57]. Substrates made from metals of the first transition group such as iron, cobalt, and nickel, are characterized by high dissolution and diffusion rates of carbon into those substrates (Table 7.3) [58]. Owing to the absence of a stable carbide layer, the incubation time required to form diamond is higher and depends on substrate thickness. In addition, these metals catalyze the formation of graphitic phases, which is reflected in the graphite-diamond ratio of during the deposition process, yielding a low diamond The importance of this mechanism in relation to diamond deposition decreases from iron to nickel, corresponding to a gradual filling of the 3d-orbital [58]. This effect occurs whenever the metal atoms come into contact with the carbon species, which can take place on the substrate or in the gas phase [59].

7.6.2 *Substrate Pretreatment*

In order for continuous film growth to occur, a sufficient density of crystallites must be formed during the early stages of growth. In general, the substrate must undergo a nucleation enhancing pre-treatment to allow this.

This is particularly true for Si wafer substrates that have been specially polished to be smooth enough for microelectronic applications. Substrates may be pre-treated by a variety of methods including:

- Abrasion with small (∼nm/μm size) hard grits (e.g., diamond, silicon carbide).
- Ultrasonication of samples in slurry of hard grit (e.g., diamond).
- Chemical treatment (acid etching and Murakami agent).
- Bias-enhanced nucleation (BEN) (negative/positive substrate biasing).
- Deposition of hydrocarbon/oil coatings.

The basis for most of these methods is to produce scratches, which provide many sites for nucleation diamond of crystallites. It is also possible that small (~ nm size) flakes of diamond, produced during abrasion with diamond grit, become embedded in the substrate, and that CVD diamond grows on this material [60].

It could be desirable to produce nucleation sites without damage to the underlying substrate. This is particularly important for some applications such as diamond electronics and optical components. One method for encouraging nucleation without damaging the substrate material has been developed: BEN.

(a) *Pretreatment on Mo/Si Substrate*

Prior to pretreatment, Si/Mo substrate are ultrasonically cleaned in acetone for 10 min to remove any unwanted residue on the surface. Abrasion with 1 μm sizes of diamond powder is performed for 5 min. Alternatively, substrate was immersed in diamond solution containing 1–3 μm of diamond particles and water for 1 h in ultrasonic bath. These methods produce scratches on the surface, which create many nucleation sites. The substrates are then washed with acetone in the ultrasonic bath for 10 min. SEM and energy-dispersive X-ray spectroscopy (EDX), characterized abraded surface of substrates.

(b) *Pretreatment on WC-Co Substrate*

The application of diamond coatings on cemented tungsten carbide (WC-Co) tools has attracted much attention in recent years in order to improve cutting performance and tool life. However, deposition of adherent high-quality diamond films onto substrates such as cemented carbides, stainless steel, and various metal alloys containing transition element has proved to be problematic. In general, the adhesion of the diamond films to the substrates is poor and the nucleation density is very low [43–49]. WC-Co tools contain 6 % Co and 94 % WC substrate with grain size 1–3 micron is desirable for diamond coatings.

In order to improve the adhesion between diamond and WC substrates, it is necessary to etch away the surface Co and prepare the surface for subsequent diamond growth. In particular, the cobalt (Co) binder; this provides additional toughness to the tool but is hostile to the diamond adhesion. The adhesion strength to diamond films is relatively poor, and can lead to catastrophic failure of coating in metal cutting [58]. The Co binder can also suppress diamond growth, favoring the formation of non-diamond carbon phases resulting in poor adhesion between the diamond coating and the substrate [61]. Most importantly, it is difficult to deposit adherent diamond onto untreated WC-Co substrates. Figure 7.2a shows sub-micron size Co crystals on diamond films that were deposited on an untreated substrate (without removal of surface Co). EDX spectra showed the trace amount of Co elements on the surface. It also showed poor adhesion of diamond film and shows delaminated film on the surface (Fig. 7.2b).

Poor adhesion can be related to the cobalt binder that is present to increase the toughness of the tool; however, it suppresses diamond nucleation and causes deterioration of diamond film adhesion. To eliminate this problem, it is usual to

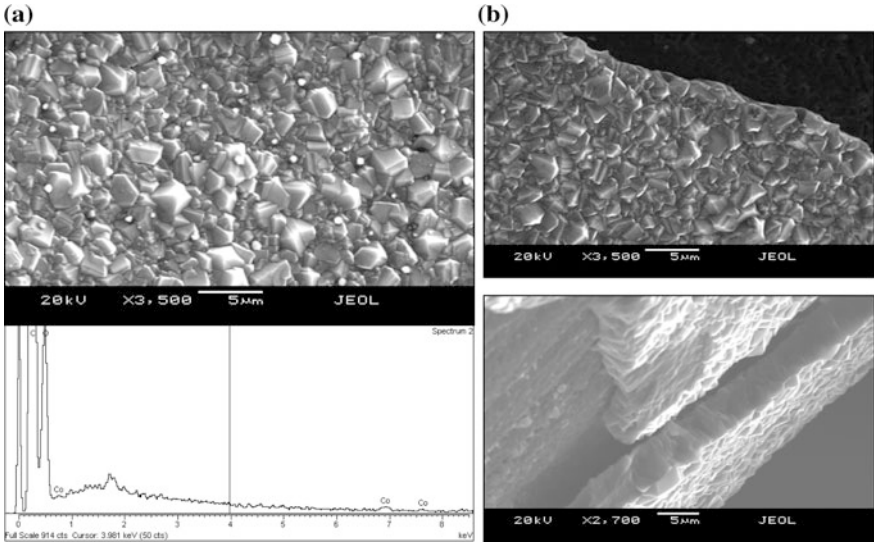

Fig. 7.2 **a** Co trace on diamond film, **b** delaminated diamond film

Table 7.4 WC-Co insert chemical composition

WC grain size (μm)	WC	Co	TaC	Density (g/cm^3)	Hardness (HRA)
WC fine grain 0.5	94.2	5.8	0.2	14.92	93.40
WC coarse grain 6	94.0	6.0		14.95	88.50

pre-treat the WC-Co surface prior to CVD diamond deposition. Various approaches have been used to suppress the influence of Co and to improve adhesion. Therefore, a substrate pre-treatment, for reducing the surface Co concentration and achieving a proper interface roughness, will enhance the surface readily available for coating process [61]. For example, chemical treatment using Murakami agent and acid etching has been used successfully for removal of the Co binder from the substrate surface [62].

The WC-Co substrates (Flat) used were 10 × 10 mm by 3 mm in thickness. The hard metal substrates used were WC-6wt% Co with WC average grain size of 0.5 μm (fine grain) and 6 μm (coarse grain). Table 7.4 shows that the data for substrate, which consist of the chemical composition, density, and hardness of samples, are used for diamond deposition. Figure 7.3a, b show that coarse and fine grain of etched WC-Co insert surface.

The Co cemented tungsten carbide (WC-Co) rotary tools (surgical tools, surgical tools), 20 mm in length including the bur head (WC-Co) and shaft (Fe/Cr) and ~1 mm in diameter, were also used. Prior to pretreatment, both set of substrates are ultrasonically cleaned in acetone for 10 min to remove any loose residues. The following two-step chemical pretreatment procedure is used. A first step etching,

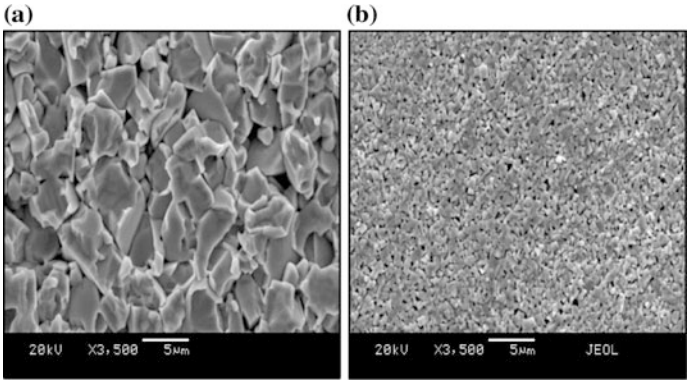

Fig. 7.3 **a** Etched coarse grain; **b** etched fine grain

using Murakami's reagent [10 g $K_3Fe(CN)_6$ + 10 g KOH + 100 ml water] is carried out for 10 min in ultrasonic bath to etch WC substrate, followed by a rinse with distilled water. The second step etching is performed using an acid solution of hydrogen peroxide [3 ml (96 % wt.) H_2SO_4 + 88 ml (30 % w/v) H_2O_2], for 10 s, to remove Co from the surface. The substrates are then washed again with distilled water in an ultrasonic bath. After wet treatment the surgical tool is abraded with synthetic diamond powder (1 μm grain size) for 5 min and followed by ultrasonic treatment with acetone for 20 min. Etched surface of substrates can be characterized by SEM and EDX.

7.7 Modification of HFCVD Process

7.7.1 Modification of Filament Assembly

The filament material and its geometrical arrangement are important factors to consider in order to have improved coatings using the CVD method. Therefore, in order to optimize both the filament wire diameter and the filament assembly/geometry, it is necessary to understand the temperature distributions of the filament. Research by the author indicated that the best thermal distribution and diamond growth uniformity is obtained using tantalum wires of 0.5 mm in diameter. To ensure uniform coating around the cylindrical shape samples (surgical tools or surgical tools), tools were positioned centrally and coaxially within the coils of the filament, the six-spiral (coil) filament was made with 1.5 mm spacing between the coils (Fig. 7.4a, b).

Tantalum wire of 0.5 mm diameter and 12–14 cm length is used as the hot filament. The filament is mounted vertically with the surgical tool held in between the filament coils, as opposed to the horizontal position used in the conventional

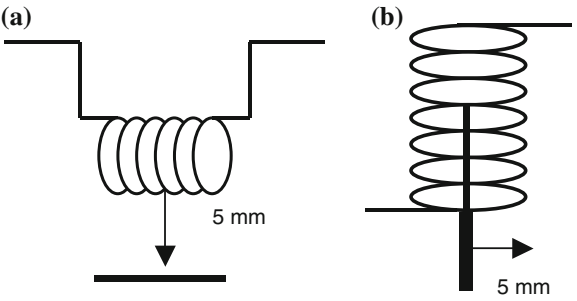

Fig. 7.4 **a** Conventional filament arrangement, **b** modified filament arrangement

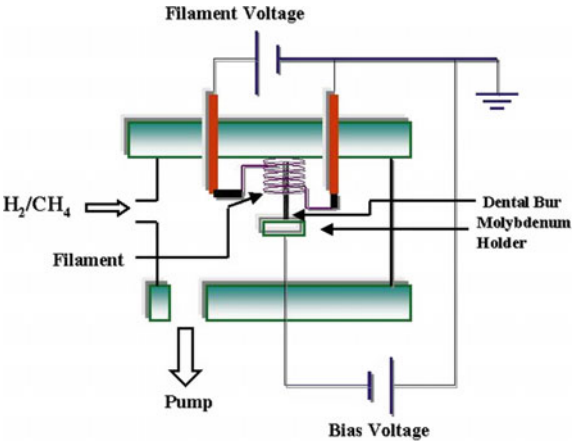

Fig. 7.5 Schematic diagram of HFCVD apparatus

HFCVD system. To ensure uniform coating, the surgical tool is positioned centrally and coaxially within the coils of the filament. A schematic diagram of the modified HFCVD system is presented in Fig. 7.5 and has been designed for surgical tool or wire or surgical tool with similar diameter. The new vertical filament arrangement used in the modified HFCVD system enhances the thermal distribution, ensuring uniform coating, increased growth rates, and higher nucleation densities.

7.7.2 Process Conditions

The CVD reactor is a cylindrical stainless steel chamber measuring 20 cm in diameter and 30 cm in length. Diamond films were deposited onto the cutting edge of the tools at 5 mm distances from the filament. The gas source used during the deposition process is composed of a mixture containing 1 % methane with excess of hydrogen; the volume flow rate for hydrogen is 100 sccm, while the volume flow rate for methane is 1 sccm. The deposition time and pressure in the vacuum chamber were 5–15 h and 20 Torr (2.66 kPa) employed. The substrate temperature

Table 7.5 Process conditions used for diamond film deposition on surgical tools

Process variables	Operating parameters
Tantalum filament diameter (mm)	0.5
Deposition time (h)	5–15
Gas mixture	1 % CH_4 in excess H_2
Gas pressure (Torr)	20 (2.66 kPa)
Substrate temperature (°C)	800–1000
Filament temperature (°C)	1800–2100
Substrate (WC-Co/Mo/Ti) diameter (mm)	Wire/drill/surgical tool (approx. 1 mm)
Distance between filament and substrate (mm)	5
Pre-treatment (Murakami etching and acid etching)	20 min plus 10 s

was measured by a K-type thermocouple mounted on a molybdenum substrate holder. The depositions are carried out between 800 and 1000 °C. The filament temperature is measured using an optical pyrometer and found to be between 1800 and 2100 °C depending upon the filament position. A summary of the process conditions is shown in Table 7.5.

7.8 Nucleation and Growth

The growth of diamond thin films at low pressures, at which diamond is metastable, is one of the most exciting developments in materials science of the past two decades. However, low growth rates and poor quality currently limit applications. Diamond growth is achieved by a variety of processes using very different means of gas activation and transport. Generalized models coupled with experiments show how process variables, such as gas activation temperature, pressure, characteristic diffusion length, and source gas composition, influence diamond growth rates and diamond quality. The modeling is sufficiently general to permit comparison between growth methods. The models indicate that typical processes, e.g., hot filament, microwave, and thermal plasma reactors operate at pressures where concentrations of atomic hydrogen, [H] and methyl radicals, [CH_3] reach maxima. The results strongly suggest that the growth rate maxima with pressure arise from changes in the gas phase concentrations rather than changes in substrate temperature.

The results also suggest that, at 1 atmospheric pressure using only hydrocarbon chemistry, growth rates saturate at gas activation temperatures above 4000 K. Models of defect incorporation indicate that the amount of sp^2, non-diamond material incorporated in the diamond is proportional to [CH_3]/[H] and therefore can be correlated with the controllable process parameters. The unusual and interesting connection between diamond nucleation and growth with the process of the vapor synthesis of diamond is essentially quite simple. Carbon-containing precursor

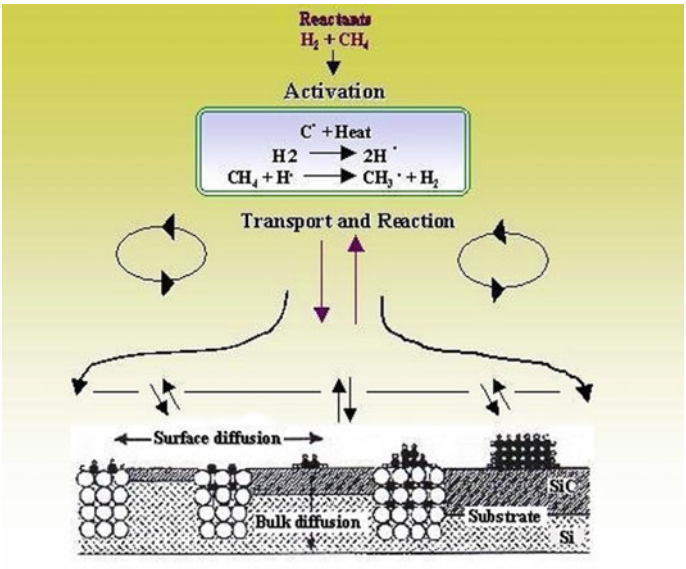

Fig. 7.6 Schematic diagram of diamond nucleation and growth

molecules (like CH_4) are excited and/or dissociated and subsequently condensing via a free dangling bond of the radical in diamond configuration on a surface [63, 64] (Fig. 7.6).

A nucleation pathway occurs through a stepwise process including the formation of extrinsic (pre-treatment) or intrinsic (in situ) nucleation sites, followed by formation of carbon-based precursors. It is believed that nucleation sites could be either grooves of scratching lines or protrusions produced by etching-re-deposition.

The gas activation is done either by hot filaments, microwave, or radio-frequency plasmas. The most crucial parameter in all this process is besides a carbon source the presence of large amounts of atomic hydrogen. The role of atomic hydrogen in the process is

- Creation of active growth sites on the surface
- Creation of reactive growth species in the gas phase
- Etching of non-diamond carbon (like graphite) graphitic, sp^2, precursors will be explored.

7.8.1 Nucleation Stage

Nucleation of diamond is a critical and necessary step in the growth of diamond thin films, because it strongly influences diamond growth, film quality and morphology [65]. Growth of diamond begins when individual carbon atoms nucleate

onto the surface to initiate the beginnings of an sp^3 tetrahedral lattice. There are two types of diamond growth:

Homoepitaxial growth: It is an application of diamond substrates, the template for the required tetrahedral structure is already there, and the diamond lattice is just extended atom-by-atom as deposition proceeds.

Heteroepitaxial growth: It uses the non-diamond substrates, there is no such template for the C atoms to follow, and those C atoms that deposit in non-diamond forms are immediately etched back to the gas phase by reaction with atomic [H].

To deal with the problem of the initial induction period before which diamond starts to grow, the substrate surface often undergoes pre-treatment prior to deposition in order to reduce the induction time for nucleation and to increase the density of nucleation sites. There are two main methods to apply this pre-treatment:

Generally, seeding or manual abrading with diamond powder or immersing in diamond paste containing small crystallites processed in an ultrasonic bath enhances nucleation. The major consideration is the nucleation mechanism of diamond on non-diamond substrates. It has been shown that the pre-abrasion of non-diamond substrates reduces the induction time for nucleation by increasing the density of nucleation sites. The abrasion process can be carried out by mechanically polishing the substrate with abrasive grit, usually diamond power of 0.1–10 μm particle size, although other nucleation methods do exist such as bias-enhanced nucleation which is used in heteroepitaxial growth. The most promising in situ method for diamond nucleation enhancement is substrate biasing. In recent years, more controlled techniques, such as bias-enhanced nucleation and nano-particle seeding, have been used to deposit smoother films [66, 67]. In this method, the substrate is biased negatively during the initial stage of deposition [67]. Before CVD diamond deposition the filament was pre-carburised for 30 min in 3 % methane with excess hydrogen to enhance the formation of tantalum carbide layer on the filament surface in order to reduce the tantalum evaporation during diamond deposition [68].

7.8.2 Bias-Enhanced Nucleation (BEN)

The substrate can be biased both negatively and positively; however, there is much research work and a large volume of literature on negative biasing. Negative substrate biasing is attractive because it can be controlled precisely; it is carried out in situ, gives good homogeneity, and results in improved adhesion. On flat substrates, such as copper and silicon, biasing has been shown to give better adhesion, improved crystallinity and smooth surfaces.

A negative bias voltage up to −300 V has been applied to the substrate relative to the filament. This produced emission currents up to 200 mA. The nucleation times used were between 10 and 30 min. In the activated deposition chamber, CH_4 and H_2 were decomposed into various chemical radical species CH_3, C_2H_2, CH_2, CH, C, and atomic hydrogen H by the hot tantalum filament. The methyl radicals

and atomic hydrogen are known to play important roles in diamond growth. In the biasing process, electrons were emitted from the diamond-coated molybdenum substrate holder and moved to the filament after they gained energy from the electrical field. When the negative bias was applied to the anode, the voltage was gradually increased until a stable emission current was established and a luminous glow discharge was formed near the substrate [69]. The nucleation density of diamond has been calculated from the SEM micrographs. Figure 7.7a, b shows the effects of bias time on the nucleation density at bias voltage of −300 V. As bias time is increased, the nucleation density also increases. The highest nucleation density was calculated to be 0.9×10^{10} cm^{-2} for a bias time of 30 min. At a bias time of 10 min, the nucleation density obtained was 2.7×10^{8} cm^{-2}.

Kim et al. [70] also reported that an increase in the emission current produced higher nucleation densities [71]. Since the bias voltage and emission current are

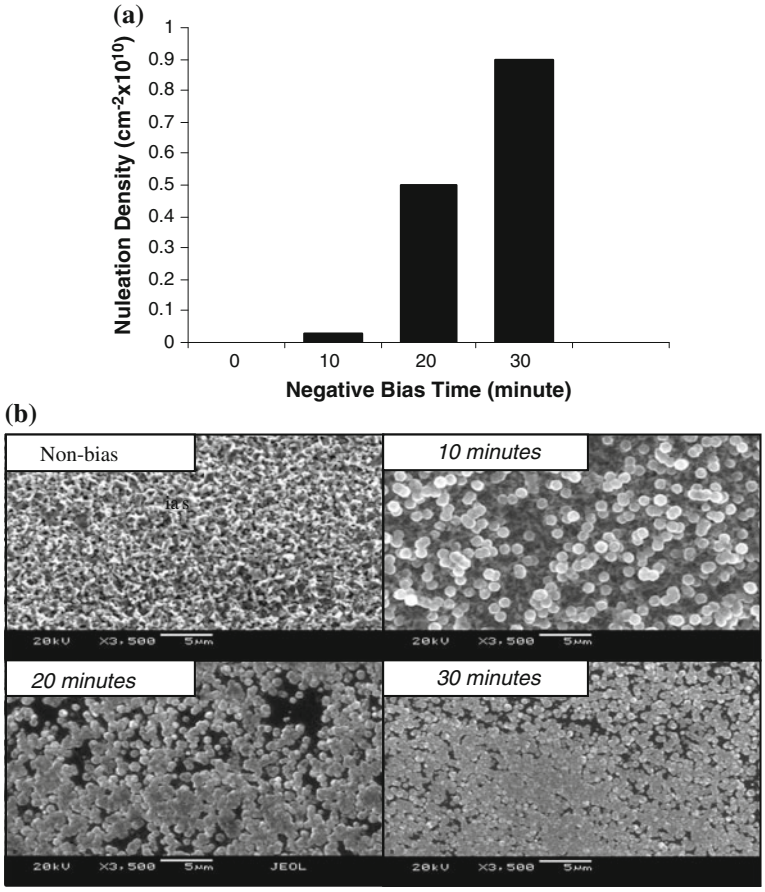

Fig. 7.7 **a** Nucleation density of diamond by BEN; **b** SEM of nucleation density on substrate

related, the enhancement of the nucleation density cannot be attributed to solely ion bombardment or electron emission of the diamond-coated molybdenum substrate holder, but may be a combination of these mechanisms [72]. Results were based on negatively BEN related to the grounded filament. However, it was reported that very low electric biasing current values (μA) were detected for applied substrate biases voltages either positive or negative. Furthermore, when increasing negative biases of up to −200 V resulted in a value of nucleation density similar to that obtained with positively BEN related to the filament. In contrast, an application of negative bias applied to the substrate at −250 V resulted in (10^{10} cm^{-2}) maximum values of nucleation density. The enhancement in the nucleation density can be attributed to the electron current from the filament by increasing the decomposition of H_2 and CH_4. The increase in the nucleation density is expected since negatively biasing the substrate increases the rate of ion bombardment into the surface creating greater numbers and density of nucleation sites. Therefore, the greater the density of nucleation sites the higher the nucleation density. Polo et al. [72] reported that reproducibility of the experiment was poor and that no definite trend in the nucleation density could be found with respect to different bias conditions.

7.8.3 *Influence of Temperature*

Temperature is a major factor in influencing the deposition rate, crystallite size, and controlling the surface roughness. Variation in the average crystallite size of diamond along the length of the substrate (surgical tool) can be attributed to the variation in the substrate temperature. The substrate temperature from the end to the center of the filament is more accentuated for molybdenum wire with a smaller diameter [9]. Figure 7.8 demonstrates the ability of this CVD process to coat 3D-shaped components, illustrating that the process is in the kinetic control regime rather than transport control regime. Most PVD type processes operate at conditions

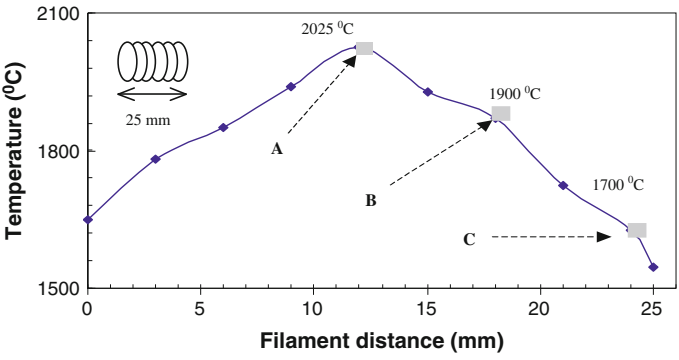

Fig. 7.8 Deposition temperature against filament position

where the rate-determining step of the deposition process is the diffusion of precursor gases to the substrate surface. Generally, this results in poor film uniformity in grooves and at the sharp edges. By operating under kinetic control regime, film uniformity is much enhanced.

Deposition temperature can also influence the diamond film thickness in terms of substrate and filament position. Analysis of temperature distribution along the coiled filament showed that the temperature is highest at the center of the filament with a rapid decrease toward the edges (Fig. 7.8). This suggests that position A is the hottest followed by position B and C on the bur. Generally, higher substrate temperatures increase diamond film growth rate and the crystallite size. At the bottom of the filament coil temperature is lower; therefore, the part of the bur parallel to the coil at this temperature will be coated with the diamond film at a lower growth rate. Therefore, it can be expected that at these regions the film will be thinner. The thermal gradient gives variations in the film thickness and crystal sizes as evident from figure. Generally, with columnar growth, the average crystallite size increases as the films become thicker. The films were thicker and the crystallite size was larger at position A compared to position C.

Analysis of temperature distribution along the coiled filament showed that the temperature is highest at the center of the filament with a rapid decrease toward the edges. The bur substrate and filament temperature have been measured parallel to the positions A, B, and C, respectively (Fig. 7.9). This suggests that position A is

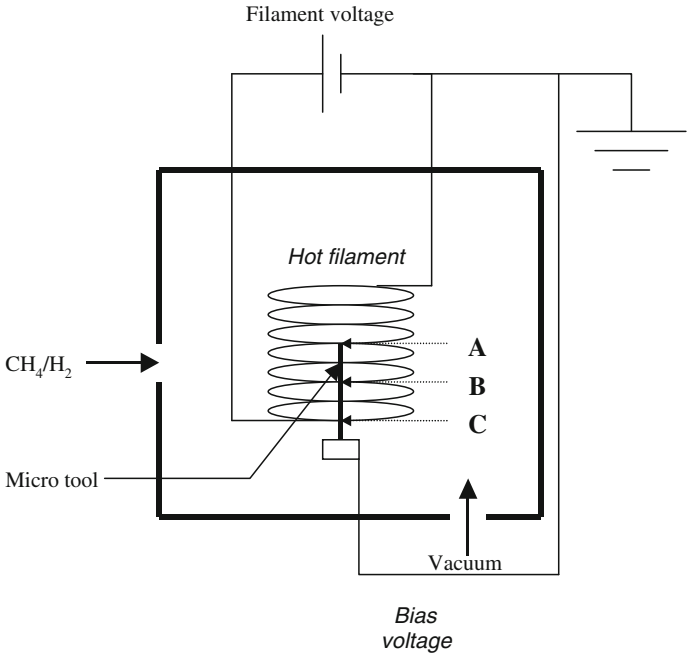

Fig. 7.9 Schematic diagram of a surgical tool assembled with filament

the hottest followed by position B and C on the bur. Variations in the film thickness and crystal sizes are mainly due to thermal gradients at various positions on the bur.

Figure 7.10 indicates that the coated surgical tool was cut in order to study the cross section of the tool. It was found that the coating is thicker at the cutting teeth

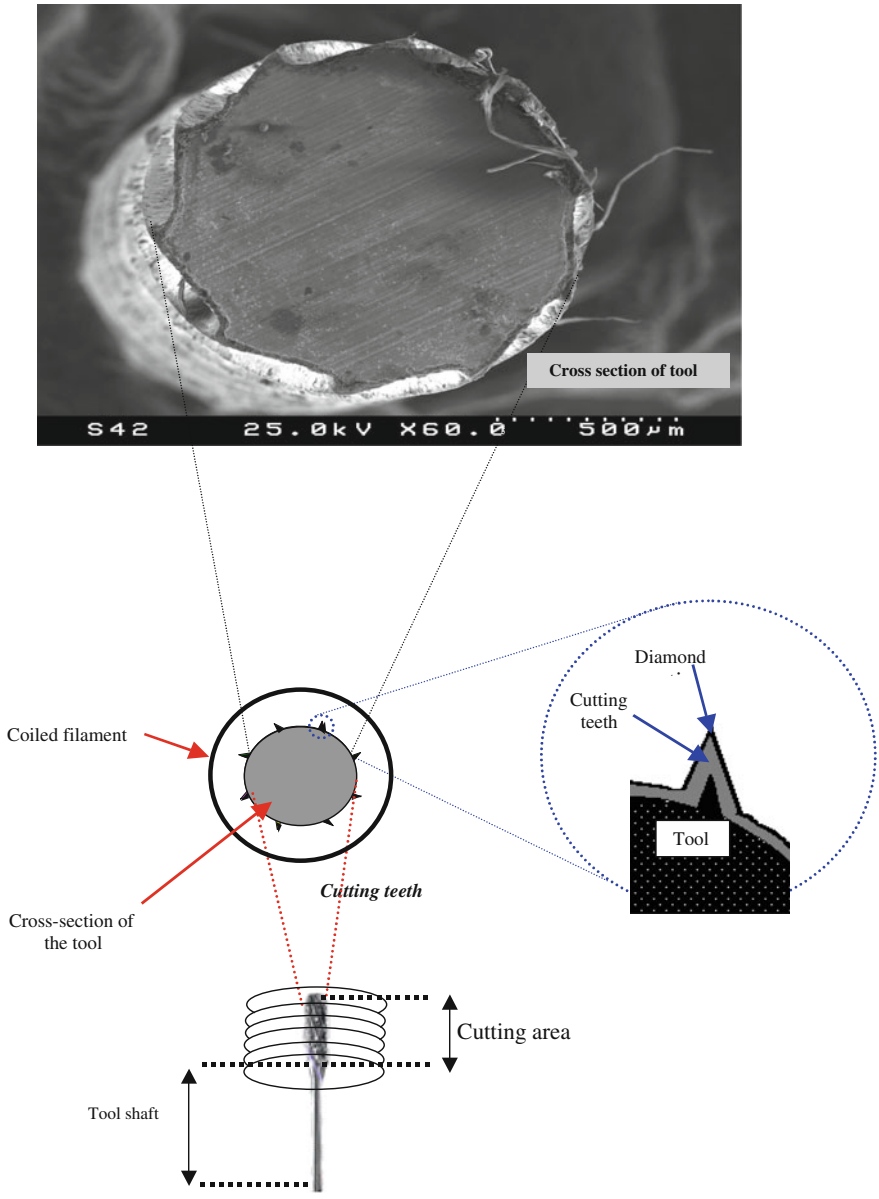

Fig. 7.10 Schematic diagram of surgical tool cutting edges

with average thickness of about 43 μm due to the slightly higher temperature at the bur tip because cutting teeth is closer to the filament coil. At the base of the bur, the heat is carried away faster and therefore it is at a lower temperature giving rise to lower growth rates and hence thinner films, at about 23 μm in thickness. Thicker coating at the tip is expected to give the tool longer life. Further work is required to study the effects of film thickness at the tooth tip and at the base on tool performance and lifetime.

Deposition temperature can also influence the diamond film thickness in terms of substrate and filament position. Analysis of temperature distribution along the coiled filament showed that the temperature is highest at the center of the filament with a rapid decrease toward the edges (Fig. 7.8). This suggests that position A is the hottest followed by position B and C on the bur. Generally, higher substrate temperatures increase diamond film growth rate and the crystallite size. At the bottom of the filament coil temperature is lower; therefore, the part of the bur parallel to the coil at this temperature will be coated with the diamond film at a lower growth rate. Therefore, it can be expected that at these regions the film will be thinner. The thermal gradient gives variations in the film thickness and crystal sizes as evident from figure. Generally, with columnar growth, the average crystallite size increases as the films become thicker. The films were thicker and the crystallite size was larger at position A compared to position C.

Analysis of temperature distribution along the coiled filament showed that the temperature is highest at the center of the filament with a rapid decrease toward the edges. The bur substrate and filament temperature have been measured parallel to the positions A, B, and C, respectively (Fig. 7.9). This suggests that position A is the hottest followed by position B and C on the bur. Variations in the film thickness and crystal sizes are mainly due to thermal gradients at various positions on the bur.

7.9 Deposition on 3D Substrates

7.9.1 Diamond Deposition on Metallic (Molybdenum) Wire

It is difficult to deposit CVD diamond onto cutting tools, which generally have a 3D shape and possess complex geometry and sharp edges, using a single step growth process [73]. The cylindrical shape wire, which has complex geometry, can be used as a model application for deposition of diamond on cutting tools such as surgical tools and surgical tools. The molybdenum (Mo) wires are deposited with CVD diamond by modified vertical filament approach. After deposition time of 5 h, continuous films of 5 μm thick CVD diamond were obtained (Fig. 7.11). The film morphology showed that it has good uniformity and high purity of diamond. The Raman spectroscopy confirmed that sp^3 diamond peak at wave number 1332.6 cm^{-1} as shown on Fig. 7.12.

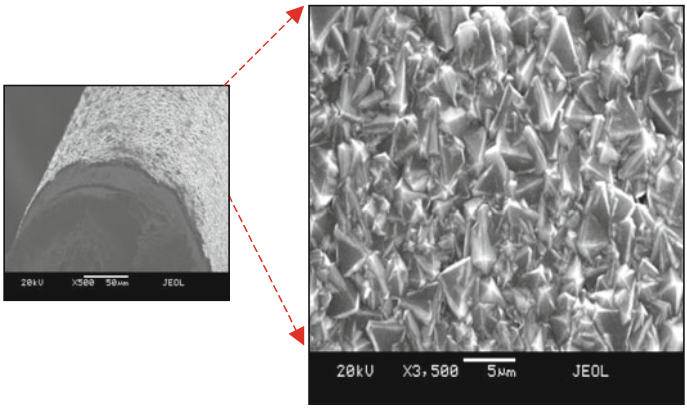

Fig. 7.11 Diamond film on molybdenum

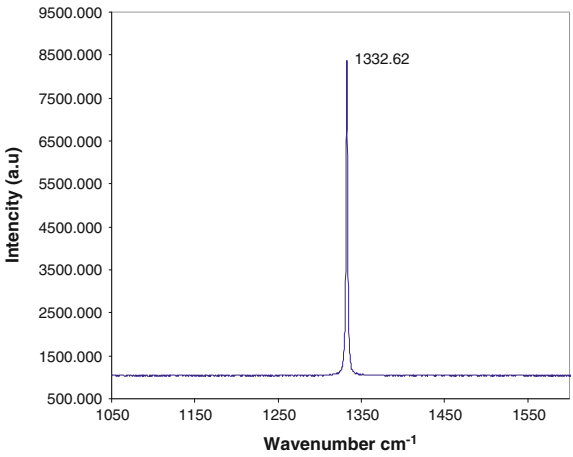

Fig. 7.12 Raman spectra of CVD diamond on molybdenum wire

7.9.2 Deposition on WC-Co Surgical Tool

Deposition of diamond on wires can be readily extended to surgical tools used for machining tool, NEMS, and MEMS devices. The uniform and adherent coating are essential in order to obtain an improved performance. Figure 7.13a shows an SEM micrograph of an uncoated surgical tool. The WC-Co cutting edges are welded onto the steel shaft (Fe–Cr). The cutting tip is 4 mm in length and 0.8 mm in diameter. The surgical tool has six sharp cutting edges, which is clearly visible in Fig. 7.13b.

Figure 7.14 shows the SEM micrographs and the corresponding EDX spectra of the WC-Co surgical tool before and after the chemical etching process. Before

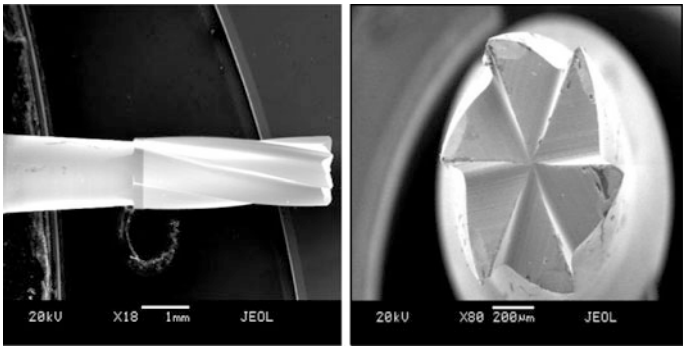

Fig. 7.13 Tip and cutting edge of surgical tool

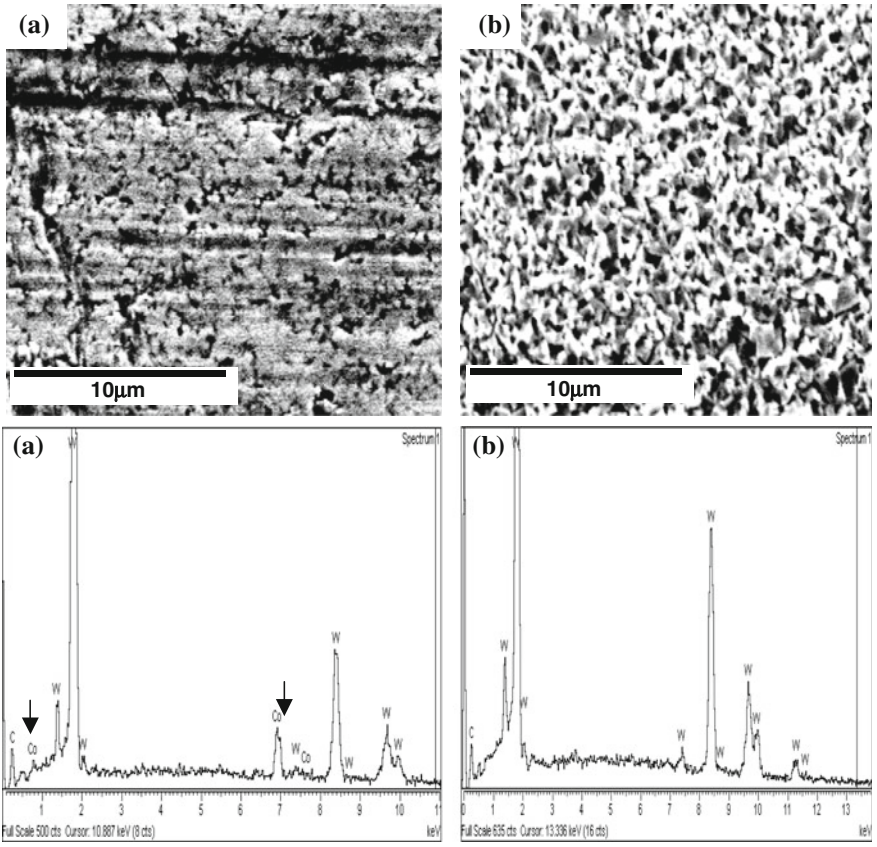

Fig. 7.14 **a** SEM and EDX of WC-Co surgical tool before etching; **b** WC-Co surgical tool after etching

etching, the EDS spectrum (Fig. 7.14a) shows the peaks for cobalt (Co), carbon (C), and tungsten (W). High cobalt content inhibits diamond deposition, resulting generally in graphitic phases, which degrade the coating adhesion. The Co diffuses to the surface regions, preventing effective bonding between the substrate surface and the film coating. To improve the coating adhesion of diamond on WC-Co tools, several approaches can be employed. For example, first, the use of interlayer material such as chromium can act as a barrier against cobalt diffusion during diamond CVD. Second, the cobalt from the tool surface can be etched using either chemical or plasma methods. Third, the cobalt can be converted into stable intermediate interlayer cobalt compounds. These can act as a barrier to cobalt diffusion from the substrate during film growth [74]. Murakami solution followed by H_2SO_4/H_2O_2 etch can be used to chemically remove the cobalt from the bur surface. The EDX spectrum shows that the Co peak has disappeared after etching. This will prove to be beneficial in enhancing the coating adhesion. Comparison of the SEM micrograph in Figs. 7.14a, b shows that the surface topography is significantly altered after etching in Murakami and H_2SO_4/H_2O_2 solutions. The etching process makes the surface much rougher with a significant amount of etch pits, which act as low-energy nucleation sites for diamond crystal growth.

An SEM micrograph of a diamond-coated WC surgical tool is shown in Fig. 7.15. Six cutting edges of the surgical tool tip were coated with a PCD film using the modified vertical HFCVD method. Analysis of the SEM picture shows that the coating uniformly covered the cutting edges as well as the nearby regions in which the placement of the surgical tool within the coils of the filament, ensuring uniform deposition. The diamond crystal structure and morphology are uniform and adherent, as shown in Fig. 7.15a, b. It also shows a close-up view of the diamond-coated region of the surgical tool in Fig. 7.15c.

Typically, the crystallite sizes are of the order 5–8 μm. The visibly adherent diamond coatings on the WC-Co surgical tools consist of mainly (111) faceted diamond crystals. The design of the filament and substrate in the reactor offer the possibility of uniformly coating even larger diameter cylindrical substrates.

Raman analysis was performed in order to evaluate the diamond carbon-phase quality and film stress in the deposited films. The Raman spectrum in Fig. 7.16 shows a single peak at 1335 cm^{-1} for the tip of the diamond-coated surgical tool. The Raman spectrum also gives information about the stress in the diamond coatings. The diamond peak is shifted to a higher wave number of 1335 cm^{-1} than that of natural diamond peak 1332 cm^{-1} indicating that stress, which is compressive in nature, exists in the resultant coatings [74].

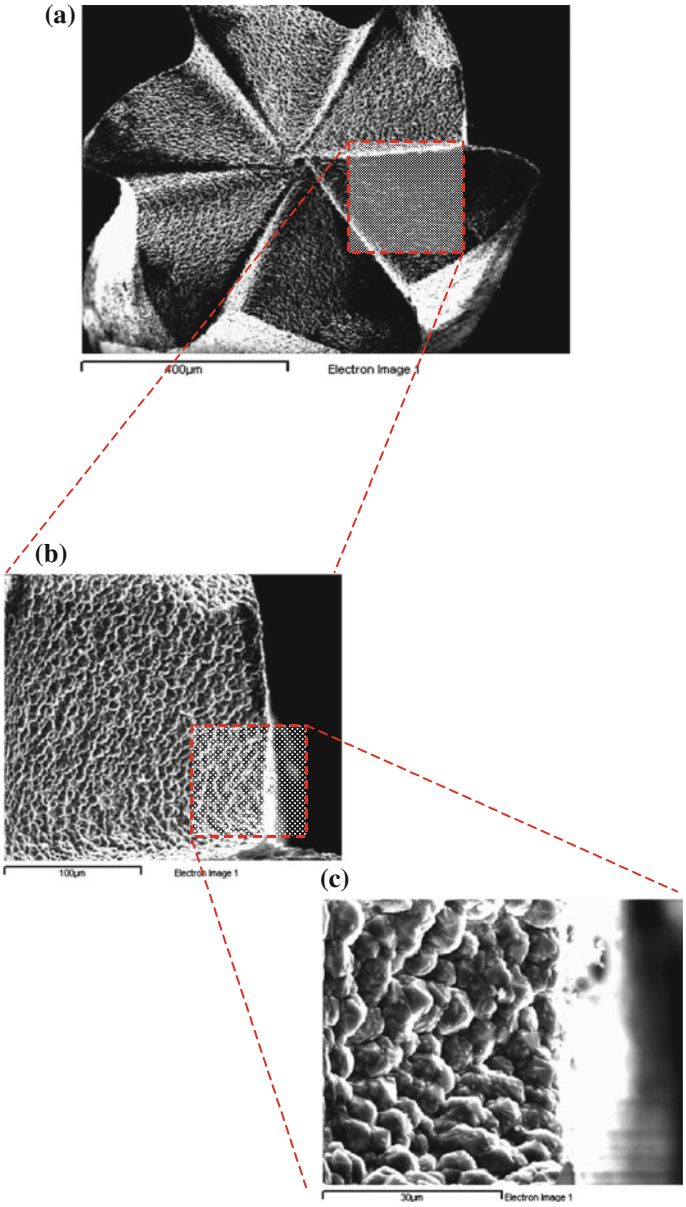

Fig. 7.15 **a** Cutting edge of surgical tool after depositing with CVD diamond; **b** cutting edge of surgical tool uniformly coated with diamond; **c** SEM of surgical tool after coating with diamond

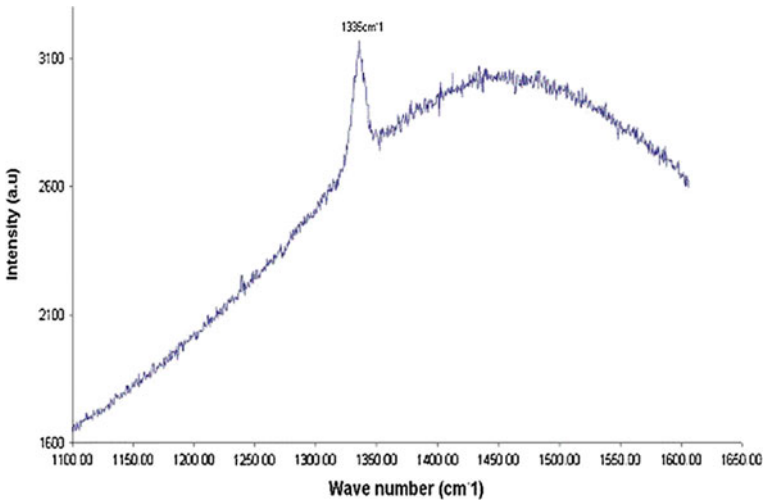

Fig. 7.16 Raman spectra of diamond-coated WC-Co surgical tool

7.9.3 Diamond Deposition on Tungsten Carbide (WC-Co) Surgical Tool

Laboratory grade tungsten carbide (WC-Co) surgical tools are shown in Fig. 7.17a, b (AT23 LR) with fine WC grain sizes (1 μm) 20–30 mm in length and 1.0–1.5 mm in diameter [supplied by Metrodent Ltd, UK] that are used for the CVD diamond deposition process.

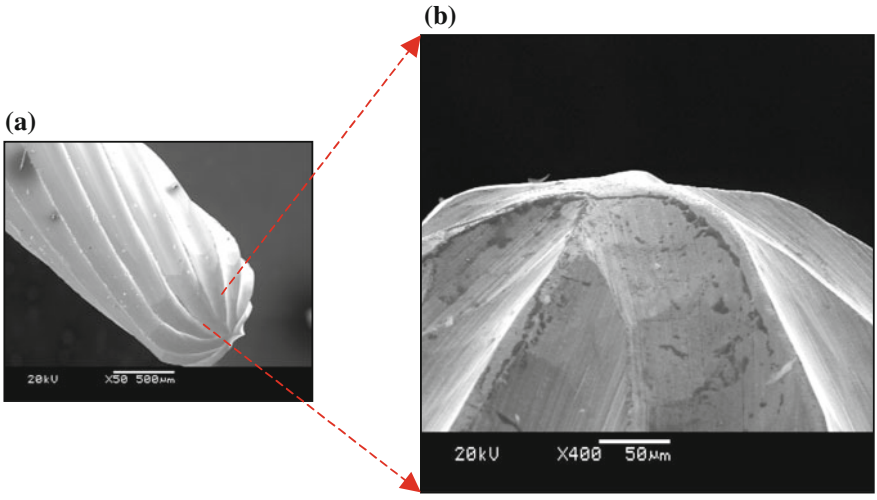

Fig. 7.17 **a** Laboratory used WC-Co surgical tool; **b** laboratory used WC-Co surgical tool before surface treatment

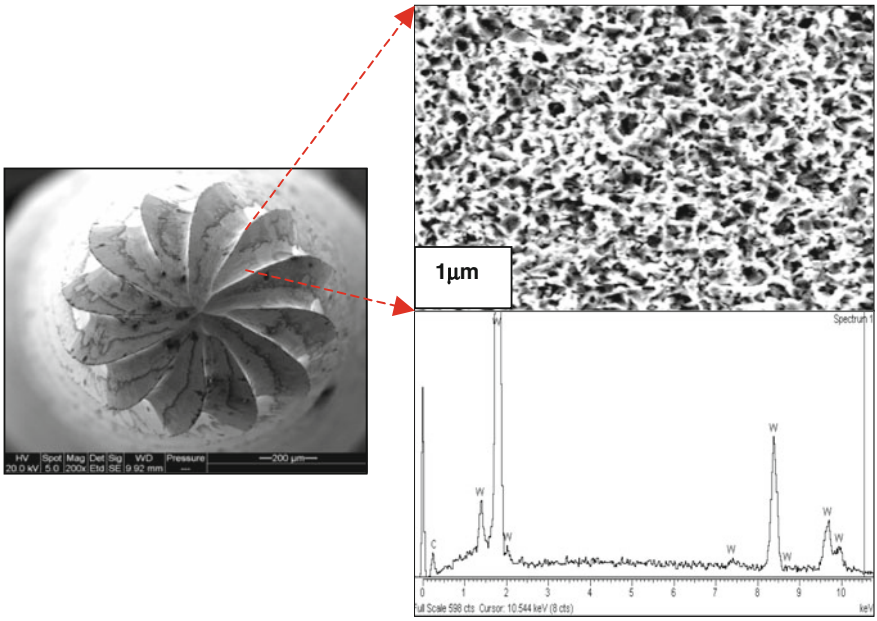

Fig. 7.18 Etched surgical tool surface after chemical treatment

The WC surface has etched away with Murakami solution and surface Co has been removed by acid etching followed by ultrasonically washing in distilled water. The EDX results confirmed that there is no indication of Co left on the surface of the etched surgical (Fig. 7.18). Diamond films have been deposited onto the cutting edge of the tools at a 5 mm distance from the tantalum wire filament.

Surface morphology of predominantly (111) faceted octahedral-shaped diamond films was obtained. The film thickness was measured to be 15–17 µm after diamond deposition for 15 h. Figure 7.19 shows the SEM micrograph of a CVD diamond-coated surgical tool (AT 23LR) at the cutting edge. The film is homogeneous with uniform diamond crystal sizes, typically in the range of 6–10 µm. As expected, the surface morphology is rough making the surgical tools extremely desirable for abrasive applications.

The Raman spectra shown show that at the tip, center, and end of cutting tool single sharps peak at 1336, 1336, and 1337 cm^{-1}, respectively, were observed for different positions (Fig. 7.20). The Raman spectrum also gives an indication about the stress in the diamond coating. The diamond peak is shifted to a higher wave number of magnitude such as 1336, 1337 cm^{-1} than that normally experienced in an unstressed coating where the natural diamond peak occurs at 1332 cm^{-1} thus indicating that the stress is compressive.

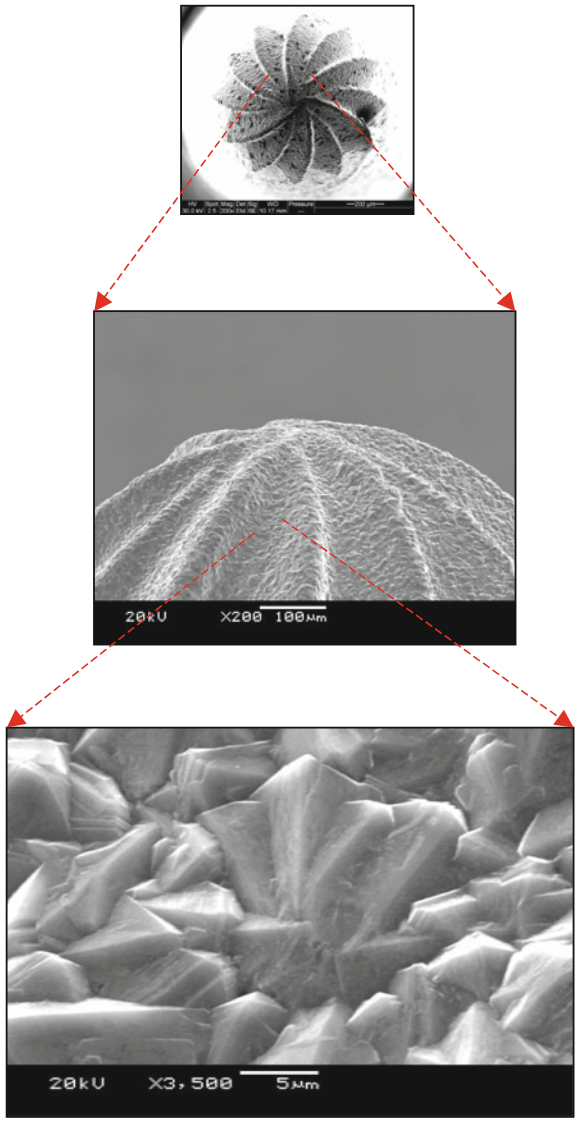

Fig. 7.19 (111) faceted octahedral shape diamond films on a surgical tool

7.10 Wear of Diamond

The quality and economy of industrial production processes are to a great extent determined by the selection and the design of appropriate manufacturing operations. For many machining operations, especially for the technologically relevant processing of metallic materials, machining with geometrically specified cutting edge is applicable. Enhancing the performance of machining operations is therefore an

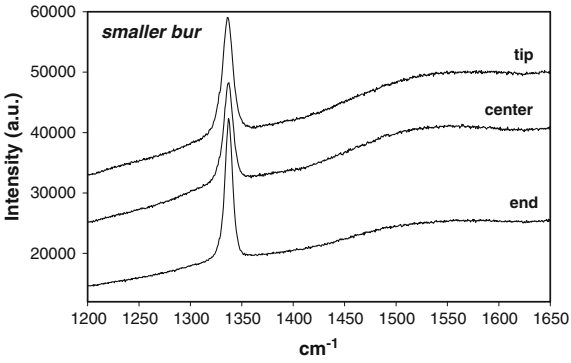

Fig. 7.20 Raman spectra of diamond film on surgical tool

economically important goal; to achieving this, coating technology can contribute in varying ways. The cutting tool is the component that is most stressed, and therefore limits the performance in NEMS and MEMS operations. Thermal and mechanical loading affects the cutting tool edges in a continuous or intermittent way. As a result, in addition to good wear resistance, high thermal stability and high mechanical strength are required for cutting materials. Opposing this objective of an ideal cutting material is the fundamental contradiction of properties hardness, strength at elevated temperature, and wear-resistance on one hand, and bending strength and bending elasticity on the other hand.

Cutting materials for extreme requirements (for example, interrupted cuts or machining of high strength materials) consequently cannot be made from one single material, but may be realized by employing composite materials.

Surface coatings may improve the tribological properties of cutting tools in an ideal way and therefore allow the application of tough or ductile substrate materials, respectively.

The coated surgical tools have been used to machine a number of materials including copper, aluminum, and iron alloys. The coated tools were compared with uncoated surgical tools to distinguish them in terms of their machining behavior. A micro-machining unit was specifically constructed at Purdue University by Professor Mark Jackson for such a purpose with a maximum spindle speed of 500,000 rpm, feed rates of between 5 and 20 μm per revolution, and cutting speeds in the range 100–200 meters per minute [75]. The micro-machining unit is shown in Fig. 7.21. The machining center is constructed using three principal axes each controlled using a D.C motor connected to a Motionmaster^{TM} controller. A laser light source is focused onto the rotating spindle in order to measure the speed of the cutting tool during machining. Post machining analysis was performed using a scanning electron microscope to detect wear on the flanks of the cutting edges.

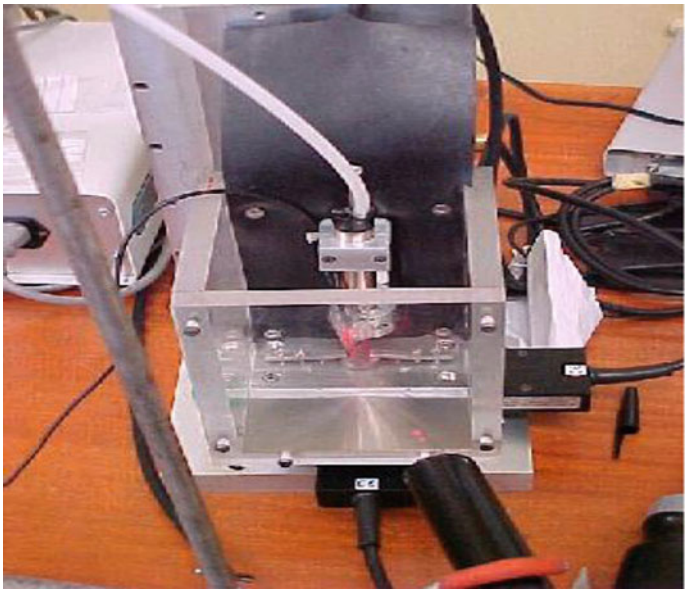

Fig. 7.21 Micro-machining center

7.10.1 Performance of Diamond-Coated Surgical Tool

After machining an aluminum alloy material, very low roughness and chipping of the diamond-coated surgical tool were detected. Figure 7.22 shows a typical machined surface in aluminum alloy. A metal chip created from this machining operation is shown in Fig. 7.23. The chip clearly shows shear fronts separated by lamellae caused by plastic instabilities within the material generated at such high speeds. Diamond-coated tools and uncoated were compared by drilling a series of holes in the aluminum alloy. The wear of each tool was determined by examining the extent of flank wear. Uncoated tools appeared to chip at the flank face, and diamond-coated tools tended to lose individual diamonds at the flank face. Uncoated tools drilled an average of 8000 holes before breakdown occurred, and the diamond-coated tools drilled an average of 24,000 holes [76].

7.10.2 Performance of Diamond-Coated Surgical Tool

In order to examine the cutting performance of the diamond-coated surgical tools machining materials such as borosilicate glass, acrylic teeth, and natural human teeth were used. Machining unit was set up for the laboratory bur (AT23LR supplied by Metrodent, UK), which used to operate at 20,000–30,000 rpm with a feed rate of 0.2–0.5 mm/rev without water-cooling.

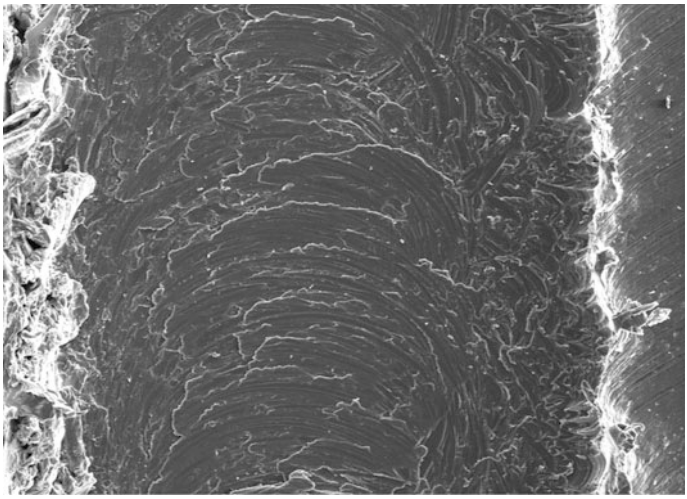

Fig. 7.22 Aluminum alloy material showing a machined track produced by a diamond-coated surgical tool

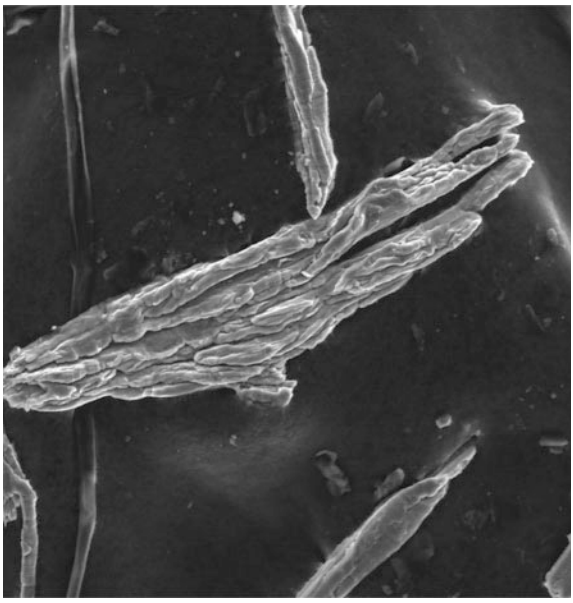

Fig. 7.23 Aluminum alloy chips generated during high-speed micro-machining operations using a diamond-coated surgical tool

The flank wear of the burs were estimated by SEM analysis at selected time interval of 1 and 3 min. Prior to SEM analysis diamond-coated burs were ultrasonically washed with 6 M Sulfuric acid solution to remove any unwanted machining material, which eroded onto surface of CVD diamond-coated bur. For comparison, the commonly used conventional PCD sintered burs with different

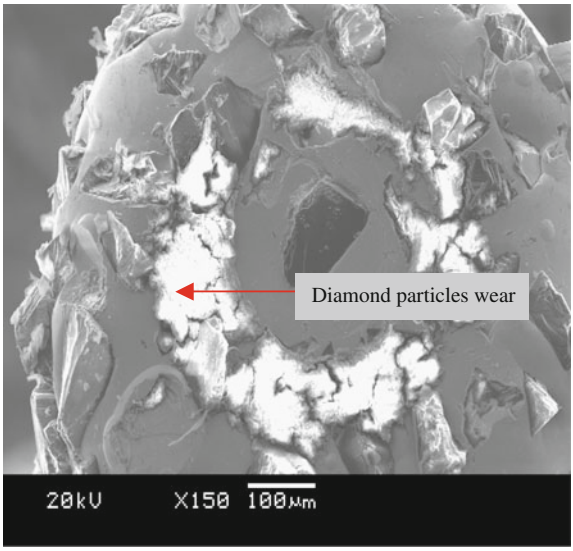

Fig. 7.24 Morphology of sintered diamond surgical tool after machining glass

geometry were also tested on the same machining materials. These burs are made by imbedding synthetic diamond particles into a nickel matrix material to bond the particles at the cutting surfaces.

The morphology of a sintered diamond bur after being tested on borosilicate glass at a cutting speed of 30,000 rpm for 5 min with an interval at every 30 s is shown in Fig. 7.24. It is clearly evident that there is significant removal of diamond particles from the surface of the tool after 500 holes. As expected, there is the deterioration of the abrasive performance of the PCD sintered diamond surgical tools.

SEM images of sintered diamond surgical tool tested on borosilicate glass (Fig. 7.24) and CVD diamond-coated laboratory bur after machining tests on borosilicate glass and acrylic/porcelain teeth, respectively, for 5 min at a cutting speed of 30,000 rpm are shown in Figs. 7.25 and 7.26. After machining, the diamond films are still intact on the pretreated WC substrate and diamond coating displayed good adhesion. There is no indication of diffusive wears after the initial test for 500 holes.

However, it was observed that the machining of materials such as glass pieces is eroded to cutting edge of the diamond surgical tool as adhesive wear (Fig. 7.25). After testing on acrylic teeth, the mechanism of wear probably involves adhesion as well as abrasion. Figure 7.26 shows that inorganic fillers from acrylic teeth adhered to the cutting tool surface in localized areas when a higher rate of abrasion was used [77].

A micrograph of an uncoated WC-Co surgical tool tested on the borosilicate glass using the same machining conditions are shown in Fig. 7.27a, b. The uncoated WC-Co bur displayed flank wear along the cutting edge of the bur. The areas of flank wear were investigated at the cutting edge of the surgical tool. A series of machining experiments have been conducted using uncoated, diamond-coated surgical tools, and sintered diamond burs when machining extracted human tooth, acrylic tooth, and borosilicate glass. The life of the burs in the machining sense was compared by using the amount of flank wear exhibited by

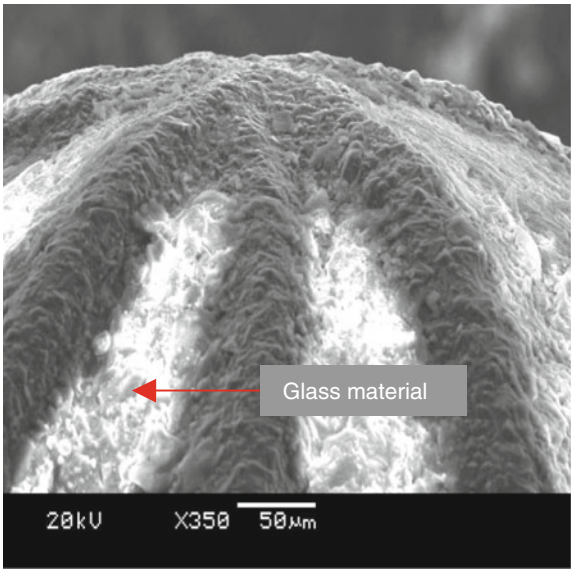

Fig. 7.25 Diamond-coated surgical tool after machining glass

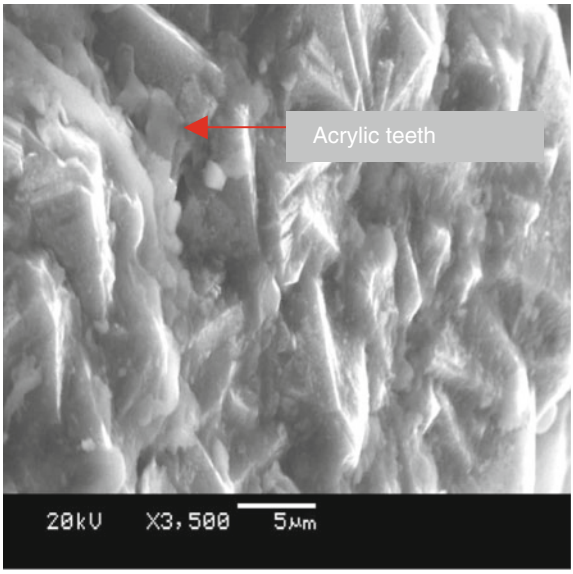

Fig. 7.26 Diamond-coated surgical tool after machining acrylic

each type of surgical tool. The flank wear was measured at time intervals of 2, 3, 4, 5, 6, and 7 min machining duration. Again, the surgical tools were examined using optical and scanning electron microscopic techniques and observed similar trends with burs that were used in drilling experiments.

The measurements of flanks wear for each bur that machined different dental materials are shown in Figs. 7.28, 7.29, and 7.30. It is evident that a longer duty

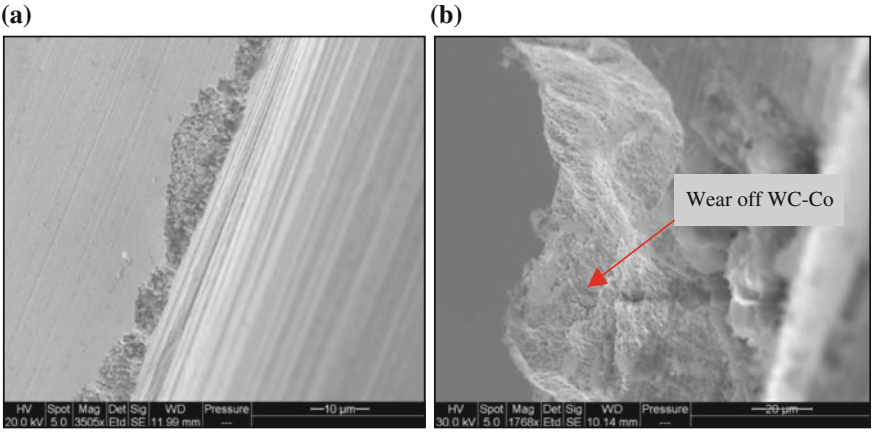

Fig. 7.27 **a** Cutting edge of WC-Co surgical tool after machining glass; **b** close-up view of WC-Co surface of the surgical tool

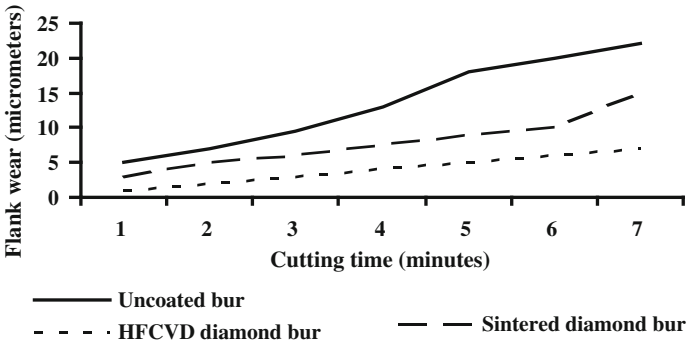

Fig. 7.28 Flank wear of cutting tools when machining borosilicate glass

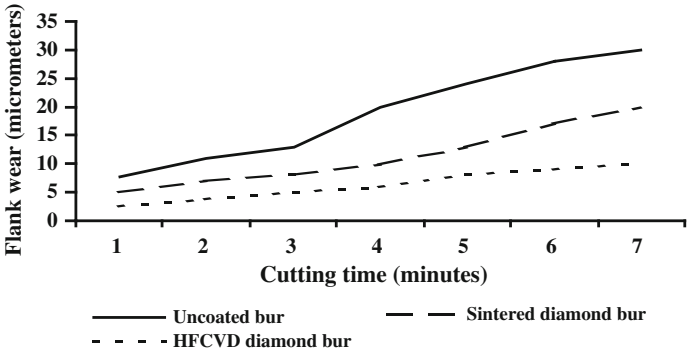

Fig. 7.29 Flank wear of cutting tools when machining acrylic material

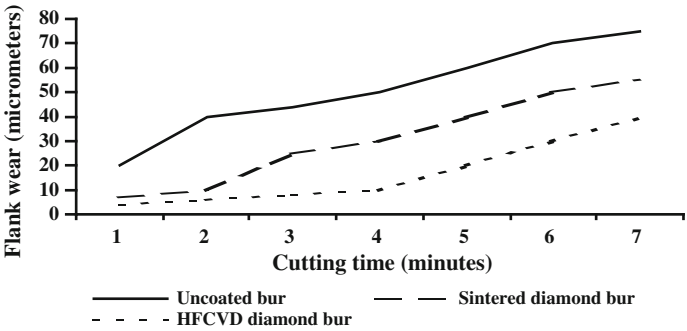

Fig. 7.30 Flank wear of cutting tools when machining dentine/enamel

cycle of machining could cause higher rate of flank wear on the cutting edge of tool. Therefore, the cutting edge of WC-Co surgical tool should have significant thickness of CVD diamond, which will enhance not only quality of cutting but will also prolong the tool life.

7.11 Time-Modulated CVD Diamond

In the conventional HFCVD method, using the relatively short bias voltage pulses in bias-enhanced nucleation in which the CH_4 concentration is increased, the flow of CH_4 during film growth is kept constant. Diamond growth in a CVD vacuum reactor is conventionally performed under constant CH_4 flow, while the excess flow of hydrogen is kept constant throughout the growth process. In developing the new TMCVD process it was considered that diamond deposition using CVD consists of two stages: (1) the diamond nucleation stage and (2) crystal growth stage.

Diamond grains nucleate more efficiently at higher CH_4 concentrations. However, prolonged film growth performed under higher CH_4 concentration leads to the incorporation of non-diamond carbon phases, such as graphitic and amorphous. The TMCVD process combines the attributes of both growth stages. This technique has the potential to replicate the benefits obtained by using pulsed power supplies, which are relatively more expensive to employ.

The key feature of the new process that differentiates it from other conventional CVD processes is that it pulses CH_4, at different concentrations, throughout the growth process, whereas in conventional CVD, the CH_4 concentration is kept constant, for the full growth process. In TMCVD, it is expected that secondary nucleation processes occur during the stages of higher CH_4 concentration pulses. This can effectively result in the formation of a diamond film involving nucleation stage, diamond growth, ad secondary nucleation and the cycle is repeated. The secondary nucleation phase can inhibit further growth of diamond crystallites. The nuclei grow to a critical level and then are inhibited when secondary nuclei form on

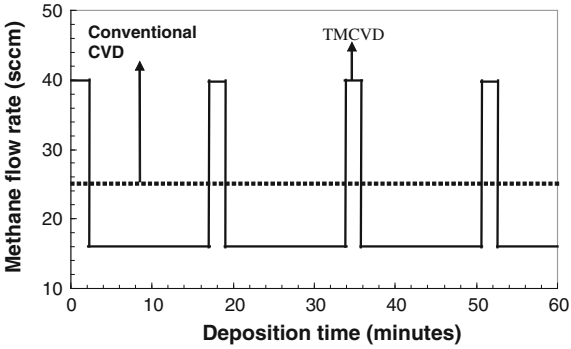

Fig. 7.31 Variations in CH_4 flow rates during film deposition in a typical time-modulated pulse cycle

top of the growing crystals and thus fill up any surface irregularities. This type of film growth can potentially result in the formation of a multilayer type film coating. In such coating systems, the quality and the surface roughness of the film coatings is dependent not on the overall thickness of the film but instead on the thickness of the individual layer of the film coating.

In demonstrating the CH_4 flow regimes, typically employed in conventional diamond CVD and TMCVD processes, Fig. 7.31 shows, as an example, the variations in CH_4 flow rates during film deposition. In the CH_4 pulse cycle employed in Fig. 7.31, the CH_4 flow rate remained constant throughout the conventional CVD process at 25 sccm. It is important to note that the hydrogen flow rate remains constant under both growth modes. CH_4 modulations at 12 and 40 sccm for 15 and 2 min, respectively, were performed during the TMCVD process using the microwave CVD system. Since higher CH_4 content in the vacuum chamber results in the incorporation of non-diamond carbon phases in the film, such as graphitic and amorphous, and degrades the global quality of the deposited film, the higher CH_4 pulse duration was kept relatively short. The final stage of the time-modulated process ends with a lower CH_4 pulse. This implies that hydrogen ions will be present in relatively larger amount in the plasma and these will be responsible for etching the non-diamond phases to produce a good quality film.

Figure 7.32a, b displays the close-up cross-sectional SEM images of diamond films grown using TMCVD and conventional CVD processes. The conventional MCD film displays a columnar growth structure. However, the time-modulated film displayed a somewhat different growth mode. Instead, the cross section consisted of many coarse diamond grains that were closely packed together. A pictorial model of the mechanism for the TMCVD process is depicted in Fig. 7.32c as compared with the conventional CVD process (Fig. 7.32d). Primarily, diamond nucleation occurs first in both the TMCVD and conventional CVD processes. However, in TMCVD, diamond nucleates more rapidly as a result of the high CH_4 pulse at the beginning. The high CH_4 pulse effectively ensures the diamond grains to nucleate quicker to form the first diamond layer. The second stage, in which CH_4 content is reduced to a lower concentration, the diamond crystallites are allowed to grow for a relatively longer period. This step enables the crystals to grow with columnar growth

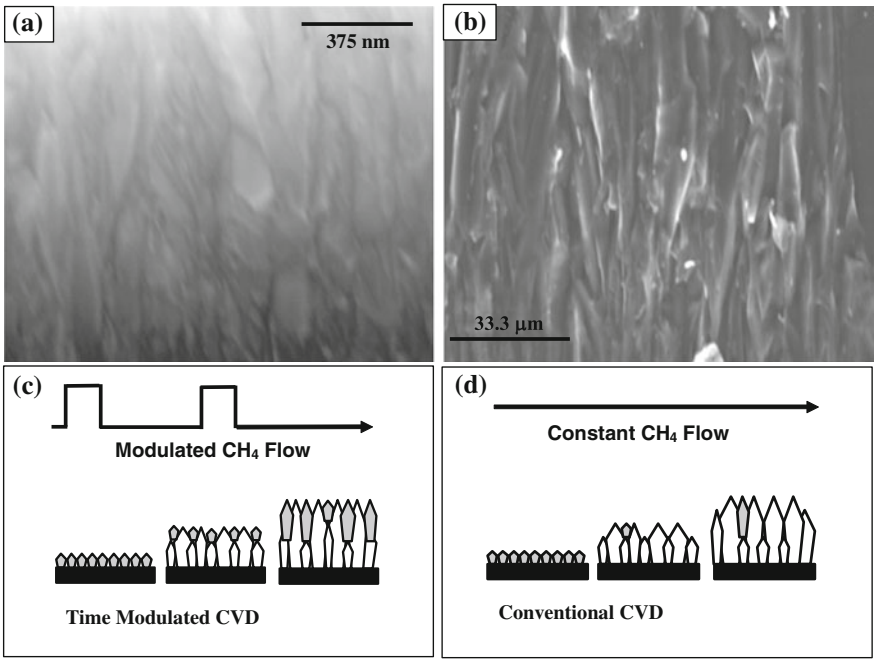

Fig. 7.32 Close-up cross-sectional SEM images of diamond films grown using **a** TMCVD and **b** conventional CVD processes. In addition, the pictorial mechanisms for film growth using TMCVD (**c**) and conventional CVD (**d**) processes are also shown

characteristics. The surface profile of the depositing film becomes rough, as expected. The third stage involves increasing the CH_4 flow back to the higher pulse. This enables further secondary nucleation of NCD to occur in between the existing diamond crystals, where the surface energy is lower. As a comparison, much less secondary nucleation occurs when the CH_4 flow is kept constant throughout the growth process. The distinctive feature of the TMCVD process is that it promotes secondary diamond-particle nucleation to occur on top of the existing grains in order to fill up any surface irregularities. Figure 7.33 displays the SEM micrograph showing secondary nucleation occurring after a high CH_4 pulse. This result justifies the proposition of the mechanism for the TMCVD process, as shown in Fig. 7.32. It can be expected that at high CH_4 bursts, carbon-containing radicals are present in the CVD reactor in greater amount, which favor the growth process by initiating diamond nucleation. The average secondary nucleation crystallite size was in the nanometer range (≤ 100 nm). It is evident that the generation of secondary nano-sized diamond crystallites has lead to the successful filling of the surface irregularities found on the film profile, in between the mainly (111) crystals. Figure 7.34 shows some randomly selected SEM images of as-deposited diamond films deposited using the TMCVD process at different CH_4 pulse duty cycles.

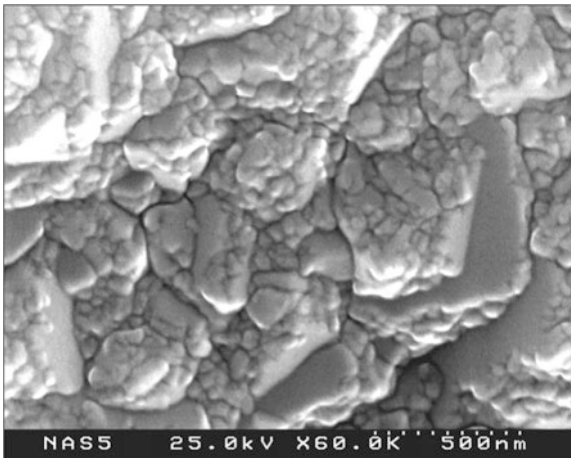

Fig. 7.33 SEM micrograph showing secondary nucleation occurring after a high CH_4 pulse

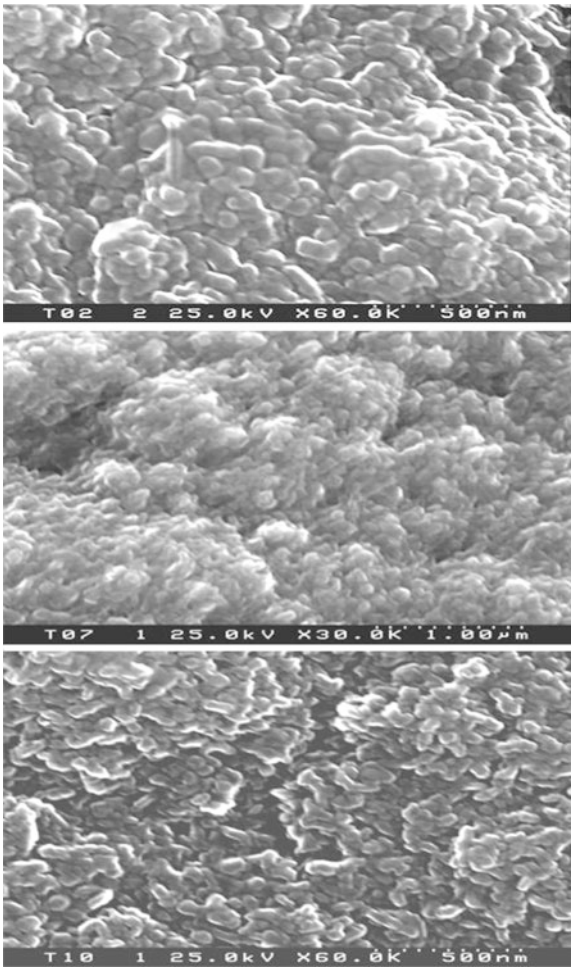

Fig. 7.34 SEM micrographs showing the morphologies of as-deposited diamond films deposited using TMCVD at different CH_4 modulation duty cycles

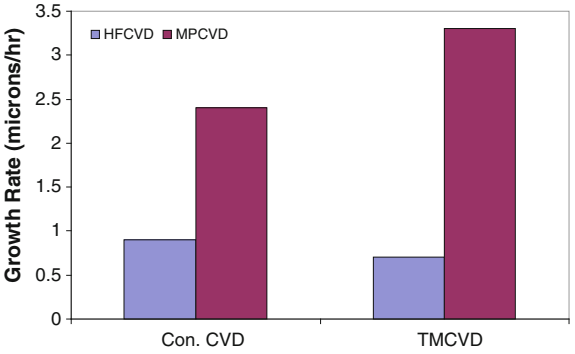

Fig. 7.35 Graph displaying the growth rates of conventional and time-modulated films grown using HFCVD and MPCVD systems

Figure 7.35 shows the graph displaying the growth rates of conventional and time-modulated films grown using HFCVD and microwave plasma CVD (MPCVD) systems. As expected, the MPCVD system gave much higher growth rates under both growth modes, conventional and time modulated, compared to films produced using HFCVD. A growth rate of 0.9 μm/h was obtained using the HFCVD system under constant CH_4 flow. The time-modulated films deposited using HFCVD were grown at a rate of 0.7 μm/h, whereas with the MPCVD system, films grown using constant CH_4 flow were deposited at a rate of 2.4 μm/h and using modulated CH_4 flow the films were grown at a rate of 3.3 μm/h. Although it is known that growth rates increase with CH_4 concentration, in the present case using the HFCVD system, the TMCVD process employs greater CH_4 flow than conventional CVD. Our results show that the growth rate of films deposited using constant CH_4 flow is slightly higher than of similar films grown using timed CH_4 modulations.

However, films grown under both modes, conventional and time modulated, using the MPCVD system produced results that were contrary to those obtained using the HFCVD system. Using the MPCVD system, the trend observed was that the films were deposited at a higher growth rate using the TMCVD process than conventional CVD. The substrate temperature is a key parameter that governs the growth rate in diamond CVD. Since the TMCVD process pulsed CH_4 during film growth, it was necessary to monitor the change in the substrate temperature during the pulse cycles. Figure 7.36 shows the graph relating substrate temperature to CH_4 concentration for both HFCVD and MPCVD systems. For the HFCVD system, it was observed that the substrate temperature decreased with CH_4 concentration. In explaining the observed trend, it needs to be considered that the dissociation of CH_4 by the hot filament absorbs energy (heat) from the filament and is considered as a cooling process. In our case the filament power was kept constant; therefore, less heat can be expected to radiate to the substrate. In addition, only a small percentage of the thermally dissociated CH species reach the substrate and transfer kinetic energy to the substrate.

It is known that the deposition of diamond films increases with substrate temperature. During the high CH_4 pulse in TMCVD, the lower substrate temperature

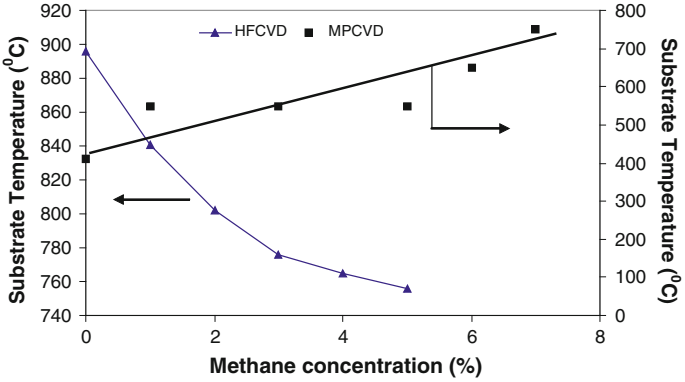

Fig. 7.36 Graph relating substrate temperature to CH_4 concentration for HFCVD and MPCVD systems

may be sufficient to lower the growth rate significantly. Generally, in a MPCVD reactor, the substrate temperature increases with CH_4 concentration, as shown in Fig. 7.36.

As a comparison, H_2 is dissociated more extensively in a MPCVD reactor than in a HFCVD reactor to produce atomic hydrogen. Furthermore, in a MPCVD reactor, the plasma power is much greater, 3400 W, than the plasma power in the HFCVD reactor. In fact, the plasma power used in MPCVD for growing diamond films was approximately 10 times greater than the power used in the HFCVD reactor. Therefore, the dissociation of CH_4 absorbs a lower percentage of the energy/heat from the plasma in a MPCVD compared to the HFCVD reactor. It is also understood that the reaction between atomic hydrogen and CH species at close proximity to the substrate releases heat. Since in a MPCVD reactor there is a greater intensity of atomic H and CH species, there will be a greater number of reactions between atomic H and CH species. This means that more heat will be released in a MPCVD reactor than in a HFCVD reactor because of such reactions.

This effect contributes to the heating of the substrate. In a HFCVD reactor, the hot filament displays much lower ability to dissociate H_2. Since atomic hydrogen is a critical species that plays an important role in producing a good quality diamond film during CVD, the quality of the films grown using HFCVD is generally lower than of similar films grown using MPCVD. In addition, the hydrogen atoms are required for the effective deposition of diamond onto the substrates. As mentioned earlier, atomic H radicals are present in greater concentration in a MPCVD reactor than in a HFCVD reactor, the MPCVD process gives higher growth rates than the HFCVD process. It is also known that by controlling the temperature during the high/low CH_4 pulse cycles, a greater number of secondary diamond grains were generated and the resultant films displayed (1) smoother surfaces and (2) higher growth rates.

7.12 Conclusions

Thin film deposition technologies, particularly CVD and PVD, have become critical for the manufacture of a wide range of industrial and consumer products. Trends in historical developments in the CVD diamond suggest that the technology is highly likely to yield substantial benefits in emerging technological products in fields of nanotechnology, biomedical engineering, NEMS, and MEMS devices. Several methods including plasma CVD, low pressure CVD, and atmospheric pressure CVD have matured into processes that are routinely used in industry. Microwave and hot filament CVD methods are now commonly used to grow diamond and these can be modified to coat uniformly for tools, NEMS, MEMS and biomedical applications. Diamond coatings examined on tools and biomedical tools showed much enhanced performance compared to uncoated tools.

References

1. Spear, K. E., & Dismukes, J. P. (1994). *Synthetic diamond: Emerging CVD science and technology*. New York: The Electrochemical Society, Wiley.
2. Wentorf, R. H. (1965). *Journal of Physical Chemistry, 69*, 3063.
3. Butler, J. E., & Woodin, R. L. (1993). *Philosophical Transactions of the Royal Society of London, A342*, 209.
4. Ashfold, M. N. R., May, P. W., Rego, C. A., & Everitt, N. M. (1994). *Chemical Society Reviews, 23*, 21.
5. Bachmann, P. K., & Messier, R. (1989). *Chemical & Engineering News, 67*, 24.
6. Spear, K. E. (1989). *Journal of American Ceramic Society, 72*, 171.
7. Joffreau, P. O., Haubner, R., & Lux, B. (1988). *Materials Research Society Symposium Proceedings, EA-15*, 15.
8. Spitsyn, B. V., Bouilov, L. L., & Deryagin, B. V. (1981). *Journal of Crystal Growth, 52*, 219.
9. Angus, J. C. (1989). *Proceedings of the Electrochemical Society, 89*, 1.
10. Yarbrough, W. A., & Messier, R. (1996). *Science, 247*, 688.
11. Messier, R., Badzian, A. R., Badzian, T., Spear, K. E., Bachmann, P. K., & Roy, R. (1987). *Thin Solid Films, 153*, 1.
12. Angus, J. C., & Hayman, C. C. (1988). *Science, 241*, 913.
13. Spear, K. E. (1989). *Journal of the American Ceramic Society, 72*, 171.
14. Kamo, M., Sato, U., Matsumoto, S., & Setaka, N. (1983). *Journal of Crystal Growth, 62*, 642.
15. Saito, Y., Matsuda, S., & Nagita, S. (1986). *Journal of Materials Science Letters, 5*, 565.
16. Saito, Y., Sato, K., Tanaka, H., & Miyadera, H. (1989). *Journal of Materials Science, 24*, 293.
17. Williams, B. E., Glass, J. T., Davis, R. F., Kobashi, K. & Horiuchi, T. (1988). *Journal of Vacuum Science Technology A* (*Vacuum, Surface, Films), 6,*1819.
18. Kobashi, K., Nishimura, K., Kawate, Y., & Horiuchi, T. (1988). *Journal of Vacuum Science Technology A* (*Vacuum, Surface, Films), 6*, 1816.
19. Liou, Y., Inspector, A., Weimer, R., & Messier, R. (1989). *Applied Physics Letters, 55*, 631.
20. Zhu, W., Randale, C. A., Badzian, A. R. & Messier, R. (1989). *Journal of Vacuum Science Technology A* (*Vacuum, Surface, Films), 7*, 2315.
21. Matsumoto, S. (1985). *Journal of Materials Science Letters, 4*, 600.
22. Matsumoto, S., Hino, M., & Kobayashi, T. (1987). *Applied Physics Letters, 51*, 737.

23. Vitkayage, D. J., Rudder, R. A., Fountain, G. G. & Markunas, R. J. (1988). *Journal of Vacuum Science & Technology A, 6*, 1812.
24. Meyer, D. E., Ianno, N. J., Woolam, J. A., Swartzlander, A. B., & Nelson, A. J. (1988). *Journal of Materials Research, 3*, 1397.
25. Wood, P., Wydeyen, T., & Tsuji, O. (1988). *Programs and Abstracts of the First International Conference on New Diamond Science and Technology, New Diamond Forum, Tokyo, Japan*.
26. Jackman, R. B., Beckman, J., & Foord, J. S. (1995). *Applied Physics Letters, 66*, 1018.
27. Suzuki, K., Sawabe, A., Yasuda, H., & Inuzuka, T. (1987). *Applied Physics Letters, 50*, 728.
28. Akatsuka, F., Hirose, Y., & Kamaki, K. (1988). *Japanese Journal of Applied Physics, 27*, L1600.
29. Suzuki, K., Sawabe, A., & Inuzuka, T. (1990). *Japanese Journal of Applied Physics, 29*, 153.
30. Niu, C. M., Tsagaropoulos, G., Baglio, J., Dwight, K., & Wold, A. (1991). *Journal of Solid State Chemistry, 91,* 47.
31. Popovici, G., Chao, C. H., Prelas, M. A., Charlson, E. J., & Meese, J. M. (1995). *Journal of Materials Research, 10*, 2011.
32. Chao, C. H., Popovici, G., Charlson, E. J., Charlson, E. M., Meese, J. M., & Prelas, M. A. (1994). *Journal of Crystal Growth, 140*, 454.
33. Postek, M. T., Howard, K. S., Johnson, A. H., & Macmichael, K. L. (1980). *Scanning electron microscopy*.
34. Kobashi, K., Nishimura, K., Kawate, Y., & Horiuchi, T. (1988). *Physical Review B, 38*, 4067.
35. Pickrell, D., Zhu, W., Badzian, A. R., Messier, R., & Newnham, R. E. (1991). *Journal of Materials Research, 6*, 1264.
36. Oatley, C. W. (1972). *Scanning electron microscope*. Cambridge: Cambridge University Press.
37. Tobin, M. C. (1971). *Laser Raman spectroscopy*. New York: Wiley Interscience.
38. Colthup, N. B., Daley, L. H., & Wiberley, S. E. (1975). *Introduction to infrared and raman spectroscopy*. New York: Academic Press.
39. Raman, C. V., & Krishnan, K. S. (1928). *Nature, 121*, 501.
40. Nemanich, R. J., Glass, J. T., Lucovsky, G., & Shroder, R. E. (1988). *Journal of Vacuum Science & Technology A, 6*, 1783.
41. Knight, D. S., & White, W. B. (1989). *Journal of Materials Research, 4*, 385.
42. Solin, S. A., & Ramdas, A. K. (1970). *Physical Review B, 1*, 1687.
43. Leyendecker, T., Lemmer, O., Jurgens, A., Esser, S., & Ebberink, J. (1991). *Surface & Coatings Technology, 48*, 253.
44. Murakawa, M., & Takeuchi, S. (1991). *Surface & Coatings Technology, 49*, 359.
45. Yaskiki, T., Nakamura, T., Fujimori, N., & Nakai, T. (1992). *Surface & Coatings Technology, 52*, 81.
46. Reineck, J., Soderbery, S., Eckholm, P., & Westergren, K. (1993). *Surface & Coatings Technology, 5*, 47.
47. Wang, H. Z., Song, R. H., & Tang, S. P. (1993). *Diamond and Related Materials, 2*, 304.
48. Inspector, A., Bauer, C. E., & Oles, E. J. (1994). *Surface & Coatings Technology, 68*(69), 359.
49. Kanda, K., Takehana, S., Yoshida, S., Watanabe, R., Takano, S., Ando, H., et al. (1995). *Surface & Coatings Technology, 73*, 115.
50. Luz, B. & Haubner, R. (1991). Diamond and Diamond-like films and coatings. In R. E. Clausing, L. L. Horton, J. C. Angus & P. Koidl (Eds.), *NATO-ISI Series B, Physics* (266, 579). NY: Plenum Press.
51. Chen, X., & Narayan, J. (1993). *Journal of Applied Physics, 74*, 1468.
52. Klass, W., Haubner, R., & Lux, B. (1997). *Diamond and Related Materials, 6*, 240.
53. Zhu, W., Yang, P. C., Glass, J. T., & Arezzo, F. (1995). *Journal of Materials Research, 10*, 1455.
54. Lux, B., & Haubner, R. (1996). *Ceramics International, 22*, 347.
55. R. C. Weast (Ed.) (1989–1990). C.R.C. *Handbook of chemistry and physics*. FL: C.R.C. Press.
56. Haubner, R., Lindlbauer, A., & Lux, B. (1993). *Diamond and Related Materials, 2*(1505), 72.

57. Chang, C. P., Flamm, D. L., Ibbotson, D. E., & Mucha, J. A. (1988). *Journal of Applied Physics, 63*, 1744.
58. Gusev, M. B., Babaey, V. G., Khvostov, V. V., Lopez-Ludena, G. M., Yu Brebadze, A., Koyashin, I. Y., et al. (1997). *Diamond and Related Materials, 6*, 89–94.
59. Endler, I., Barsch, K., Leonhardt, A., Scheibe, H. J., Ziegele, H., Fuchs, I., et al. (1999). *Diamond and Related Materials, 8*, 834–839.
60. Kamiya, S., Takahashi, H., Polini, R., & Traversa, E. (2000). *Diamond and Related Materials, 9*, 191–194.
61. Inspector, A., Oles, E. J. & Bauer, C. E. (1997). *International Journal of Refractory Metals and Hard Materials*, *15*, 49.
62. Itoh, H., Osaki, T., Iwahara, H., & Sakamoto, H. (1991). *Journal of Materials Science, 26*, 370.
63. Liu, H. & Dandy, D. S. (1996). *Diamond chemical vapor deposition*. NY: Noyes.
64. Nazare, M. H. & Neves, A. J. (1998). *Properties, growth and application of diamond.*
65. Zhang, G. F., & Buck, V. (2000). *Surface & Coatings Technology, 132*, 256.
66. May, P., Rego, C., Thomas, R., Ashfold, M. N., & Rosser, K. N. (1994). *Diamond and Related Materials, 3*, 810.
67. Gouzman, I., & Hoffmann, A. (1998). *Diamond and Related Materials, 7*, 209.
68. Wang, W., Liao, K., Wang, J., Fang, L., Ding, P., Esteve, J., et al. (1999). *Diamond and Related Materials, 8*, 123.
69. Wang, B. B., Wang, W., & Liao, K. (2001). *Diamond and Related Materials, 10*, 1622.
70. Kim, Y. K., Han, Y. S., & Lee, J. Y. (1998). *Diamond and Related Materials, 7*, 96.
71. Wang, W. L., Liao, K. J., & Gao, G. C. (2000). *Surface & Coatings Technology, 126*, 195.
72. Polo, M. C., Wang, W., Sanshez, G., Andujar, J., & Esteve, J. (1997). *Diamond and Related Materials, 6*, 579.
73. Sein, H., Ahmed, W., Rego, C. A., Jones, A. N., Amar, M., Jackson, M. J., et al. (2003). *Journal of Physics: Condensed Matter, 15*, S2961–S2967.
74. Amirhaghi, S., Reehal, H. S., Plappert, E., Bajic, Z., Wood, R. J. K., & Wheeler, D. W. (1999). *Diamond and Related Materials, 8*, 845–849.
75. Jackson, M. J., Gill, M. D. H., Ahmed, W., & Sein, H. (2003). Proceedings of the Institute of Mechanical Engineers—(Part L). *Journal of Materials, 217*, 77–83.
76. Sein, H., Jackson, M. J., Ahmed, W., & Rego, C. A. (2000). *New Diamond and Frontier Carbon Technology, 12*(6), 1–10.
77. Sein, H., Ahmed, W., Jackson, M. J., Woodwards, R., & Polini, R. (2004). *Thin Solid Films, 447–448*, 455–461.